PURIFICATION AND CHARACTERIZATION OF DIACYLGLYCEROL KINASE EPSILON

A STRUCTURAL AND ENZYMATIC CHARACTERIZATION OF PURIFIED HUMAN DIACYLGLYCEROL KINASE EPSILON

By

WILLIAM JENNINGS, B.Sc

A Thesis

Submitted to the School of Graduate Studies

In Partial Fulfillment of the Requirements for the Degree

Master of Science

McMaster University

MASTER OF SCIENCE (2016) McMaster University

(Biochemistry) Hamilton, Ontario, Canada

TITLE: The Purification and Characterization of Human Diacylglycerol Kinase Epsilon

AUTHOR: William Jennings, B.Sc. (McMaster University)

SUPERVISOR: Dr. Richard M. Epand

NUMBER OF PAGES: ix, 122

ABSTRACT

Diacylglycerol kinases (DGK's) tightly regulate the intracellular levels of diacylglycerol (DAG) and phosphatidic acid (PA). DAG is an important intermediate in lipid biosynthetic pathways and acts as a lipid second messenger in a number of signaling pathways. Similarly, since PA serves as a potent signaling lipid and is a precursor for lipid biosynthesis, intracellular PA levels must be tightly regulated. There are ten isoforms of DGK in mammals, but we have decided to focus solely on the epsilon form (DGK**ε)** in this work. DGK**ε** is the only isoform that shows specificity for the acyl chains of its DAG substrate; as a consequence, it contributes to the dramatic enrichment of cellular lipids with sn-1 stearoyl and sn-2 arachidonoyl. The most notable example is the highly enriched bioactive lipid 1-stearoyl-2-arachidonoyl phosphatidylinositol. We have purified active human DGKε to near homogeneity and thoroughly characterized its stability as well as examined its secondary structure with CD. We also purified a truncated form (DGKε Δ40) that shows increased stability compared to the full-length protein. Our purified fractions are well suited for a wide range of exciting applications and studies. We have begun incorporating DGKε into liposomes in order to develop a liposome-based assay, which would be a dramatic improvement over the presently used micelle-based assay. This purification also allows for high throughput screens of chemical compounds to test for a specific inhibitor. These studies will reveal valuable information about the structural and functional properties of DGKε and will aid in the development of therapies for DGKε-related diseases.

ACKNOWLEDGEMENTS

I sincerely thank my supervisor and mentor Dr. Richard Epand for his consistent support and encouragement throughout my thesis. He has been a patient, considerate, and knowledgeable mentor who has always made himself available to provide me with valuable advice and expertise. I am very grateful for all of the opportunities he has provided me with and for fostering my love for research.

I also thank my supervisory committee members Dr. Alba Guarné and Dr. Joaquin Ortega for their dedication to providing me with guidance and constructive feedback throughout my thesis.

I am very grateful and thankful to all of my lab members past and present who have helped me in different ways throughout my thesis. In particular, Dr. Raquel Epand, Dr. Prasanta Hota, Kenneth D'souza, Dr. José Bozelli and Sejal Doshi for their assistance and advice.

I am very thankful to Dr. Donna D'souza for her support over the latter half of my thesis, her willingness to provide valuable advice and genuine interest in helping me any way she could was much appreciated.

Lastly, I owe thanks to my family who has always supported me. My accomplishments would not have been possible without the ever-present support of my grandparents, my mother, sisters, and brother.

TABLE OF CONTENTS

LIST OF FIGURES

CHAPTER 1

CHAPTER 2

LIST OF TABLES

CHAPTER 2

PREFACE

The following work is presented as a sandwich thesis. Chapter 1 introduces the function and importance of the diacylglcyerol kinases, specifically diacylglycerol kinase epsilon. The chapter consists of a review that we published in 2015. Chapter 2 is a manuscript that we are almost ready to submit that outlines the purification of diacylglycerol kinase epsilon, as well as a partial characterization of its conformational and enzymatic properties. Chapter 3 addresses some of the many applications that can be undertaken now that diacylglycerol kinase epsilon has been purified. It discusses some of the preliminary results we have obtained with the purified enzyme, and suggests studies that can be further developed. The published review paper in chapter 1 is presented as the submitted word document. All chapters have been reproduced with consent of the authors.

CHAPTER 1: Introduction

Molecular Properties of diacylglycerol Kinase-Epsilon in Relation to Function.

William Jennings, Sejal Doshi, Kenneth D'souza, and Richard M. Epand

This paper provides an introduction to diacylglycerol kinase epsilon, its function within the cell, its structure and the nature of its interactions with its substrate and lipids. It also discusses some of the unique properties of this enzyme and its physiological relevance. My contribution to this paper was to write some of the sections and prepare all the figures with the assistance of Sejal Doshi and edit the paper. Kenneth D'souza and Richard Epand both wrote some of the sections and edited. Richard Epand was responsible for putting the manuscript together.

---

[1] Jennings, W., Doshi, S., D'Souza, K., & Epand, R. M. (2015). Molecular properties of diacylglycerol kinase-epsilon in relation to function. *Chemistry and physics of lipids*, *192*, 100-108.

[2] Reproduced with permission form Elsevier Limited

Molecular Properties of Diacylglycerol Kinase-Epsilon in Relation to Function

William Jennings, Sejal Doshi, Kenneth D'Souza and Richard M. Epand

Department of Biochemistry and Biomedical Sciences, McMaster University, 1280 Main Street West, Hamilton, Ontario L8S 4K1, CANADA

Address correspondence to: Richard M. Epand, Department of Biochemistry and Biomedical Sciences, McMaster University, 1280 Main Street West, Hamilton, Ontario L8S 4K1, CANADA; Tel. 905 525-9140; Fax 905 521-1397; E-mail: epand@mcmaster.ca

Keywords: Diacylglycerol kinase, lipid binding, lipid substrate specificity, arachidonic acid

Abbreviations: DAG, diacylglycerol; DGK, diacylglycerol kinase; DGKε, the epsilon isoform of diacylglycerol kinase; DOG, 1,2-dioleoyl-glycerol; DOPC, 1,2-dioleoyl-phosphatidylcholine; ECS, electroconvulsive shock; ER, endoplasmic reticulum; HD, Huntington disease; Htt, Huntingtin protein; KO, knockout; LTP, long term potentiation; MEF, mouse embryo fibroblast; PA, phosphatidic acid; PI, phosphatidylinositol; PI-cycle, metabolic cycle to synthesize PI; PIP_2, phosphatidylinositol-4,5-bisphosphate; PIP_n, all forms of phosphorylated PI; PKC, protein kinase C; PM, plasma membrane; P-motif, phosphate binding motif; SAG, 1-stearoyl-2-arachidonoyl-glycerol; SAPA, 1-stearoyl-2-

arachidonoyl-PA; SLG, 1-stearoyl-2-linoleoyl-glycerol; SLPA, 1-stearoyl-2-linoleoyl-PA; NMR, nuclear magnetic resonance; WT, wild-type.

Abstract:

The epsilon isoform of mammalian diacylglycerol kinase (DGKε) is an enzyme that associates strongly with membranes and acts on a lipid substrate, diacylglycerol. The protein has one segment that is predicted to be a transmembrane helix, but appears to interconvert between a transmembrane helix and a re-entrant helix. Despite the hydrophobicity of this segment and the fact that the lipid substrate is also hydrophobic, removal of this hydrophobic segment by truncating the protein at the amino terminus has no effect on its enzymatic activity.

The amino acid sequence of the catalytic segment of DGKε is highly homologous to that of a bacterial DGK, DgkB. This has allowed us to predict a conformation of DGKε based on the known crystal structure of DgkB.

An important property of DGKε is that it is specific for diacylglycerol species containing an arachidonoyl group. The region of DGKε that interacts with this group is found within the accessory domain of the protein and not in the active site nor in the hydrophobic amino terminus. The nature of the acyl chain specificity of the enzyme indicates that DGKε is associated with the synthesis of phosphatidylinositol. Defects or deletion of the enzyme give rise to several disease states.

Outline

I. Membrane Binding of DGKε

    Membrane penetration

    N-terminal hydrophobic segment

II. Comparison of DGK from bacteria and from mammals

III. Conformational properties of DGKε

    Structure of the protein

    Thermal stability

    Effects of lipids on conformation

IV. Interaction of DGKε with its lipid substrate

V. DGKε and the PI cycle

VI. Biological roles of DGKε

    DGKε regulates seizure susceptibility

    DGKε prevents cardiac hypertrophy and heart failure

    Atypical hemolytic-uremic syndrome and mutation of DGKε

VII. Summary and Future Prospective

I. Introduction

In mammals there are ten known isoforms of the enzyme diacylglycerol kinase (DGK), as well as gene splice variants. Enzymes of this family all have a homologous active site but differ widely in their molecular mass, mechanisms of activation and biological function (Shulga, Topham et al. 2011a). Among these isoforms, only the epsilon isoform of diacylglycerol kinase (DGKε) has a particularly hydrophobic segment that is predicted to be a transmembrane helix. DGKε has several unique features among all the isoforms of DGK (unless otherwise stated, DGK refers to human isoforms, although the sequence is highly conserved among all multicellular eukaryotes). DGKε is the only isoform believed to be permanently attached to a membrane. It is the smallest isoform in terms of molecular mass and it is the only form known to exhibit acyl chain specificity of the lipid substrate, diacylglycerol (DAG). DGKε shows high specificity for 1-stearoyl-2-arachidonoyl glycerol (SAG), the species of DAG with the same acyl chain composition found in the lipid intermediates of the phosphatidylinositol cycle (PI-cycle) (D'Souza and Epand ,2014). All DGK isoforms have two or three C1 domains, but the epsilon isoform is the only one that does not have any other recognizable folding domain.

In the present review we will focus on the nature of the interactions between DGKε and membranes, as well as interactions of this enzyme with its lipid substrate.

II. Membrane Binding of DGKε

Membrane Penetration

Fluorescence microscopy and sub-cellular fractionation experiments have demonstrated that DGKε in cells is bound to membranes and is localized at the endoplasmic reticulum (ER) and plasma membrane (PM) (Decaffmeyer, Shulga et al. 2008; Matsui, Hozumi et al. 2014; Kobayashi, Hozumi et al. 2007). While its localization within these membranes is not unique among DGK isoforms, DGKε is the only isoform that has been predicted and shown to be membrane bound (Decaffmeyer, Shulga, Dicu, Thomas, Truant, Topham, Brasseur, and Epand, 2008; Glukhov, Shulga et al. 2007). However, there is one report where DGKε was found on stress fibres in smooth muscle (Nakano, Hozumi et al. 2009). Interestingly, questions remain about the nature of the association of this enzyme with membranes i.e. is it peripherally associated or an integral membrane protein? It should be noted however that there is nothing fundamentally different between integral and peripheral membrane proteins. This is an arbitrary classification based on phenomenology, *i.e.* whether a protein can be extracted from a membrane without disrupting the entire membrane structure. As discussed below, DGKε does not clearly fall into one or the other of these two categories, but is rather a protein whose properties are intermediate between an integral and peripheral membrane protein.

Solubilization studies have shown that high pH or high salt conditions can extract 11% and 14%, respectively, of Flag-DGKε from membranes of COS-7 cells that over-express this protein. Buffers at physiological pH and salt concentration solubilize a

negligible amount of Flag-DGKε (Dicu, Topham et al. 2007). However, the difference between an integral and a peripheral membrane protein is based on experimental phenomenon and there may not be a clear separation between the two classes. While true integral membrane proteins cannot be extracted from membranes through high pH or salt conditions, the low extraction rates of DGKε suggest that it may be more tightly associated than a typical peripheral membrane protein. DGKε's membrane binding ability is determined by the hydrophobic N-terminal segment comprising of residues 20-42 (residue numbers in this review include the N-terminal Met as residue 1, residue numbering in some of our earlier papers did not include the N-terminal Met, since it is cleaved in the mature protein). This segment of the protein is predicted to form a transmembrane helix with a probability close to 1, according to the program **TMHMM Server, v. 2.0** (Figure 1).

Atomic Force Microscopy studies (in progress) have demonstrated that DGKε forms greater and larger aggregates on a DOPC supported lipid bilayer compared to DGKε Δ40, a truncated form of the protein which has the N-terminal hydrophobic segment (first forty residues) removed. These results are highly suggestive that the N-terminal hydrophobic segment of DGKε is a contributing factor to the observed aggregation. Similar studies have also demonstrated that the number and size of DGKε aggregates are reduced in the presence of a preferred substrate such as SAG. However, this effect is not observed with less preferred substrates such as dilinoleoylglycerol. Similar effects of SAG on aggregation were observed with DGKε Δ40. Therefore, it is

hypothesized that the preferred substrate may have a stabilizing effect on a non-aggregated and more active conformation of DGKε.

N-terminal hydrophobic segment

Deleting the hydrophobic segment of the protein does not alter the acyl chain specificity of DGKε towards arachidonoyl-containing DAG either in the case of DGKε Δ40 (Dicu, Topham, Ottaway, and Epand, 2007) or DGKε Δ58 (Lung, Shulga et al. 2009). However, this N-terminal segment does play an important role in membrane insertion.

The prediction that the segment of residues (20-42) is transmembrane is supported by experiments based on access to glycosylation in the interior of the endoplasmic reticulum of various constructs containing this N-terminal hydrophobic segment of DGKε (Norholm, Shulga et al. 2011). There is however, some evidence to suggest that this hydrophobic segment forms a re-entrant helix. This is based on the observation that when DGKε, labeled with 3X-FLAG at the amino terminus, is expressed in NIH-3T3 cells, no FLAG epitope is accessible to immunostaining on the exterior of the cell (Decaffmeyer, Shulga, Dicu, Thomas, Truant, Topham, Brasseur, and Epand, 2008). However, permeabilizing the cell membrane with detergent can access the FLAG epitope. When the Pro residue, near the center of the hydrophobic segment, at residue 33, is mutated to Ala, the FLAG epitope is exposed to the outside of the cell (Decaffmeyer, Shulga, Dicu, Thomas, Truant, Topham, Brasseur, and Epand, 2008). It is possible that the FLAG tag prevents the peptide from fully entering the membrane, although this would mean that it

only prevents the insertion of the wild type protein but not the P33A mutant. There is also a difference in the thickness and lipid composition of the endoplasmic reticulum used for the glycosylation studies (Norholm, Shulga, Aoki, Epand, and von Heijne, 2011) and the plasma membrane used for the fluorescence microscopy (Decaffmeyer, Shulga, Dicu, Thomas, Truant, Topham, Brasseur, and Epand, 2008). *In silico* analysis suggests that two families of stable conformations exist for this hydrophobic segment and that they are in equilibrium with one other. One of the conformations is a transmembrane helix and the other is a re-entrant helix. These calculations also predict that the mutant P33A would be largely a transmembrane helix as found (Decaffmeyer, Shulga, Dicu, Thomas, Truant, Topham, Brasseur, and Epand, 2008). It is possible that there is equilibrium between these two conformational forms that can be influenced by relatively small changes in the system such as the nature of the surrounding lipid or interactions with other proteins.

The transmembrane segment may be critical for the exchange of DGKε between the ER and the PM. Subcellular fractionation experiments of WT DGKε vs. the P33A mutant reveal that while the majority of WT protein is within the entire ER fraction, the P33A mutant appears to be restricted towards the lighter ER fractions (Decaffmeyer, Shulga, Dicu, Thomas, Truant, Topham, Brasseur, and Epand, 2008). How these changes affect the physiological function of DGKε is currently unknown.

The N-terminal hydrophobic segment also may play a role in the self-association of DGKε. Studies using PFO-PAGE show that DGKε forms a roughly 50:50% mixture of monomers and dimers (Dicu, Topham, Ottaway, and Epand, 2007). However, when the

first 40 amino acids are deleted (including the hydrophobic segment), DGKε Δ40 primarily forms monomers.

III. Comparison of DGK from bacteria and from mammals

Bacteria express two forms of DGK; DgkA and DgkB. DgkA is an integral membrane protein comprised of three transmembrane alpha helices. It is capable of phosphorylating DAG and other lipids such as ceramide (Van Horn, Kim et al. 2009; Van Horn and Sanders, 2012). DgkA is amongst the smallest known kinases, and is a homotrimer that is structurally distinct from other kinases. The sequence, membrane topology and substrate specificity of DgkA is unique among DGKs from all species. There are two families of DgkA, those from Gram positive bacteria and those from Gram negative bacteria. The DgkA from Gram positive bacteria is primarily an undecaprenol kinase, while DgkA from Gram negative bacteria is a DAG-kinase (Jerga, Lu et al. 2007). DgkA from the Gram negative bacteria, *E. coli,* also catalyzes the transfer of phosphate from ATP not only to lipid species, but also to molecules of water and glycerol (Ullrich, Hellmich et al. 2011; Prodeus, Berno et al. 2013). A study using ^{31}P NMR to detect ATP hydrolysis and DAG phosphorylation was used to investigate ATPase activity of human DGKε and determine if water competes with DAG as an acceptor of the γ phosphate of ATP as is seen with DgkA (Prodeus, Berno, Topham, and Epand, 2013). The results indicate that with human DGKε, water does not compete with DAG for the γ phosphate of ATP. Essentially all of the γ phosphate of ATP is transferred to the lipid substrate and there is no detectable production of inorganic phosphate resulting from ATPase activity

(Prodeus, Berno, Topham, and Epand, 2013). This work suggests that in the evolution of DGK from bacteria to mammals, the phosphoryl transfer reaction became more efficient and specific with the exclusion of water and glycerol. Furthermore, the work revealed that the substrate specificity of human DGKε is not a consequence of different degrees of ATP hydrolysis in the presence of different species of DAG (Prodeus, Berno, Topham, and Epand, 2013). Since mammalian DGKε shows minimal ATPase activity, and is specific for DAG species with acyl chain compositions that are also predominant in PI species (stearoyl and arachidonoyl), it is believed to be committed to PI re-synthesis and acyl chain enrichment (D'Souza and Epand, 2014).

A second bacterial DGK is the water soluble DgkB found in gram-positive bacteria. DgkB forms a tight homodimer, and each monomer is believed to be capable of independently supporting substrate binding and catalysis (Miller, Jerga et al. 2008). DgkB shares 15%-18% sequence identity with the human DGKs and its catalytic site is conserved in all mammalian DGKs. In comparison, the DGK found in yeast is less closely related to mammalian DGKs, and uses CTP as the phosphate donor as opposed to ATP (Han, O'Hara et al. 2008). Another distinction between DGK expressed in multicellular organisms versus bacteria and yeast is that multicellular organisms express several DGK isoforms to fulfill unique biological functions specific to multicellular organisms, such as brain function and immune response. To date, ten mammalian DGK isoforms have been identified, which can be grouped by common structural elements into five subfamilies. Like the DGKs found in other multicellular eukaryotes, all of the mammalian isoforms have at least two cysteine-rich, C1 domains and a catalytic domain

(Shulga, Topham, and Epand, 2011a). Of the ten mammalian isoforms of DGK, only DGKε has the unique property of being specific for DAG species with particular acyl chains. NCBI's BLAST reveals that human DGKε is homologous to forms from a wide variety of multicellular eukaryotes; the top 100 hits consist entirely of DGKε from various multicellular eukaryotes. Unsurprisingly, human DGKε is nearly 100% identical to a variety of primate species.

IV. Conformational properties of DGKε

Structure of the protein

Currently no crystal structures exist for any of the mammalian DGK isoforms. However, there is a crystal structure reported for the bacterial DgkB from *Staphylococcus aureus* (Miller, Jerga, Rock, and White, 2008). Miller et al. show that the key active site residues in DgkB and the components of an associated Asp•water•Mg^{2+} network that extends toward the active site locale are conserved in the catalytic sites of mammalian DGKs (Miller, Jerga, Rock, and White, 2008). The conservation of key active site residues and the Asp•water•Mg^{2} across prokaryotic and eukaryotic organisms indicates that the DGK in these organisms use the same catalytic mechanism and have similar structures (Miller, Jerga, Rock, and White, 2008). A sequence alignment of DGKε and DgkB reveals 18% amino acid sequence identity and the majority of this corresponds to their active site regions (Soding, 2005). All of the mammalian DGKs have an evolutionarily conserved catalytic domain with a conserved *GGDG* sequence known as the phosphate-binding motif (P-motif). The *GGDG* sequence is conserved in several protein kinase families including the 6-fructokinases, NAD kinases, as well as in DgkB

(Abe, Lu et al. 2003). Interestingly, the *GGDG* motif is not found in DgkA, although there is some sequence homology in this region between DgkA and DGKε (Figure 2). Despite the active site being highly conserved among all forms of DGK, except, DgkA, the structures of DGKε and DgkB are quite distinct beyond the active site region. For example, DgkB is comprised of 20% alpha helix content and 31% beta strand content, while DGKε is predicted to possess 18% of both alpha helices and beta strands according to the PSIPRED server (Buchan, Minneci et al. 2013; Jones, 1999). I-TASSER predicts alpha helix content to be 25% and beta strand content to be 21% for DGKε (Roy, Kucukural et al. 2010; Yang, Yan et al. 2015; Zhang, 2008). Despite the minor difference in overall secondary structure content, the predicted topology of these elements is in very good agreement between these two predictive algorithms. In addition, our initial experiments suggest that the overall secondary structure of DGKε measured by CD, agrees well with that found for the crystal structure of DgkB. The I-TASSER server used the structures of four bacterial proteins, including an alcohol dehydrogenase and three DgkBs, a melB apo-protyrosinase from *Aspergillus oryzae*, and a human sphingosine kinase as templates to generate the structure depicted in Figure 3 (Roy, Kucukural, and Zhang, 2010; Yang, Yan, Roy, Xu, Poisson, and Zhang, 2015; Zhang, 2008). Of the templates used, the one with the highest structural similarity is *Staphyloccus aureus* DgkB (Roy, Kucukural, and Zhang, 2010; Yang, Yan, Roy, Xu, Poisson, and Zhang, 2015; Zhang, 2008). Figure 3A shows the domain that has some homology to that of lipoxygenase, that we suggest is responsible for forming close contacts with the arachidonoyl group (orange colour) is in a location in the structure that would allow the

OH group of SAG to reach the active site (red). The orange motif is also consistent with its location allowing entry of the substrate into the interior of the protein, in analogy with lipoxygenase binding of arachidonic acid. However, the secondary structure folding patterns of this domain is very different in the two proteins (see Section V for additional discussion of the lipoxygenase motif). Another feature of the DGKε structure that can be discerned from Figure 3B is that the conformation of the hydrophobic amino-terminal segment is the only segment of several amino acid residues whose position is not well defined (estimated accuracy ~14 Å).

NCBI's pBLAST alignment of the bacterial DgkB and human DGKε amino acid sequences generates three regions of overlap. Interestingly, the aligned region corresponding to residues 274 to 373 of DGKε and residues 62 to 147 of DgkB have matching secondary structure elements. Furthermore, despite the primary structures not aligning, the secondary structure of the first 61 residues in DgkB matches that of DGKε from residues 213 to 273. Thus, the local folding of the first 147 residues of DgkB matches that of human DGKε between residues 213 to 373 (Buchan, Minneci, Nugent, Bryson, and Jones, 2013; Jones, 1999) (Figure 4). This alignment suggests that the secondary structure pattern is generally more conserved that the primary structure. To further examine this region in the two enzymes, a 3D structure prediction of DGKε generated using the I-TASSER server was compared to the previously determined DgkB crystal structure (Figure 5). The folding of this region is quite similar between the two enzymes, and a 3D alignment shows that these regions can be superimposed onto one another (Figure 5). It should be noted that two of the five 3D structures generated by I-

TASSER align much better with DgkB, so we have chosen to include one of them in Figure 5. Furthermore, the alpha helices making up the catalytic domain of DGKε are amphipathic (Figure 6A) just as they are in DgkB. The model in Figure 6B shows that the amino terminal hydrophobic segment is not well integrated into the protein structure, but remains separated. Therefore it is not surprising that we have found this segment to not play a role in enzyme activity or in acyl chain specificity; but instead it is well suited for insertion into a lipid bilayer or interaction with another protein. The active site of DGKε is in a hydrophobic region of the protein and could therefore bind the hydrophobic lipid substrate with the exclusion of water, preventing the enzyme from catalyzing any ATPase activity. However, the active site does have some charged residues that may facilitate the binding of ATP (Figure 7).

Domain 1 of DgkB is comprised of the first 124 amino acid residues as well as the C-terminal residues 286-315 (Miller, Jerga, Rock, and White, 2008). This domain contains the active site and shows a high degree of structural homology to mammalian DGKs, including DGKε (Figure 5). However, domain 2 of DgkB appears to have been lost during evolution, while new elements were simultaneously acquired to allow for additional specific functions in the larger mammalian enzymes.

Thermal stability and effect of lipids on the conformation of DGKε

Circular Dichroism spectroscopy indicates that the secondary structure content of DGKε and the truncated form, DGKε Δ40, of the enzyme are nearly identical. DGKε exhibits a gradual and irreversible loss of secondary structure on heating to 100°C, with slight stabilization upon the addition of small unilamellar vesicles of dioleoyl-

phosphatidylcholine (DOPC). In contrast, DGKε Δ40 retained less structure at 100°C and showed a cooperative denaturation at approximately 80°C with DOPC present (work in progress). Interestingly, DGKε interacts with DOPC differently than DGKε Δ40 does; yet both experience a stabilizing effect from the lipid at higher temperatures. Mixed micelle activity assay experiments have demonstrated that glycerol has a significant stabilizing effect on DGKε during storage at 4°C and -80°C, as well as during freeze/thaw cycles.

V. Interaction of DGKε with its lipid substrate

A major component of the interaction between DGKε and lipid bilayers is the insertion of the hydrophobic segment comprising residues 20-42 into the membrane, as discussed above. However, this is not the only interaction of this protein with lipids. One of the substrates of DGKε, DAG, is also a lipid (the other substrate being ATP). DGKε is highly specific towards DAG substrates that contain an arachidonoyl moiety. Because there is a similar pattern of amino acid residues required for both DGKε (Shulga, Topham, and Epand, 2011b) and certain lipoxygenases (Neau, Gilbert et al. 2009), we have suggested that part of the interaction of DGKε with its lipid substrate occurs with the region of the protein containing this amino acid pattern. We have termed this amino acid pattern as the LOX motif and have defined it as L-$X_{(3-4)}$-R-$X_{(2)}$-L-$X_{(4)}$-G, in which -$X_{(n)}$- is *n* residues of any amino acid.

This segment is found within the accessory domain of DGKε, corresponding to residues 436-456. It is not found in other mammalian DGK isoforms. This segment is

critically required for DGKε's enzymatic activity and acyl chain specificity (Shulga, Topham et al. 2011b). Located at the N-terminus of this segment is a conserved LOX motif corresponding to L431-G443. The crystal structure of 8R-lipoxygenase suggests that these essential residues form part of a channel that provides access to the catalytic site (Neau, Gilbert et al. 2009). Mutating any of the conserved residues of the LOX-motif affects both enzymatic activity and arachidonoyl specificity of DGKε (Shulga, Topham, and Epand, 2011b). Mutations that we made in the LOX motif of DGKε resulted in proteins largely devoid of enzymatic activity and hence it was difficult to characterize the residual activity of the mutants. We therefore mutated a segment of DGKε adjacent to the LOX-motif that caused a smaller decrease in enzyme activity, and in two cases (Y451F and R457Q) the mutations resulted in an unexpected increase in enzymatic activity (D'Souza and Epand ,2012). These mutations are more hydrophobic, which may facilitate better alignment between the hydroxyl group of the substrate and the catalytic site of DGKε. The high residual activity of these and other mutations in the region of DGKε between residues 447 and 457 resulted in changes in preference between arachidonoyl and linoleoyl-containing substrates (D'Souza and Epand, 2012). The native form of DGKε has a preference for SAG over 1-stearoyl-2-linoleoyl glycerol (SLG) as substrate. This preference can be either increased or decreased by mutation in this region of the protein. We suggest that because the segment 447-457 is adjacent to the LOX-motif, mutations in this region do not drastically eliminate substrate binding, but they do modify the substrate binding pocket in a manner that affects relative substrate specificity.

VI. DGKε and the PI-cycle

It should be noted that DGKε is not highly expressed in all tissues (it is most prevalent in the brain, retina, and cardiac muscle), yet PI can still be synthesized and enriched with specific acyl chains by other processes (D'Souza, Kim et al. 2014; Milne, Ivanova et al. 2008). However, in tissues such as the brain, where there is high DGKε expression, there is a particularly large amount of acyl chain enrichment with *sn-1* stearoyl and *sn-2* arachidonoyl species of PI (D'Souza and Epand, 2014). Studies using DGKε KO MEFs demonstrate the importance of DGKε in the PI-cycle by showing that there is roughly a three-fold reduction in PA and PI content in the plasma membrane of these cells compared to the plasma membrane of WT MEFs (Shulga, Myers et al. 2010). Similar lipodomic studies with DGKε KO MEFs show significant differences in the levels of arachidonate-containing glycerophospholipids between WT and KO cells (Milne, Ivanova, Armstrong, Myers, Lubarda, Shulga, Topham, Brown, and Epand, 2008). The lipid class showing the greatest reduction in arachidonoyl content is the phosphoinositides (PI and PIPn) (Milne, Ivanova, Armstrong, Myers, Lubarda, Shulga, Topham, Brown, and Epand, 2008). DGKε KO cells show the greatest reductions in the levels of 38:4 PI, corresponding to 1-stearoyl-2-arachidonoyl phosphatidylinositol. Other lipid classes also show reduced arachidonoyl content, although the effect on PI is greatest (Milne, Ivanova, Armstrong, Myers, Lubarda, Shulga, Topham, Brown, and Epand, 2008). As expected, these lipidomic studies show that in DGKε KO cells, the enrichment of arachidonoyl content from DAG to PA is decreased as expected from the loss of the arachidonoyl-specific DGKε. Unexpectedly, the arachidonoyl enrichment from PA to PI

is also decreased, although DGKε does not catalyze any reaction in this path. Thus DGKε may also be involved in another function to increase enrichment of arachidonoyl content during the conversion of PA to PI (Milne, Ivanova, Armstrong, Myers, Lubarda, Shulga, Topham, Brown, and Epand, 2008) which we are currently investigating.

VII. Biological Roles of DGKε

DGKε regulates seizure susceptibility

DGKε's involvement in PI-synthesis and acyl chain enrichment makes it an important component in several signalling pathways. It appears to have a particularly important role in neural function (D'Souza and Epand, 2014). Targeted deletion of DGKε in mice was shown to reduce levels of free arachidonic acid, 20:4-DAG, and 20:4-PI(4,5)P_2 in response to electroconvulsive shock (Lukiw, Cui et al. 2005; Musto and Bazan, 2006; Bazan, 2005). These lipids serve several important biological functions and their dysregulation is implicated in a range of diseased states. Phospholipids act as reservoirs of free 20:4, which is converted to prostaglandins during epileptogenesis. It is also known that 20:4 DAG accumulates in the brain during seizures (Bazan, 2005; Horrocks and Farooqui, 1994; Sun, Xu et al. 2004; Aveldano and Bazan, 1975; Bazan, Morelli de Liberti et al. 1982). Physiologically, the DGKε-KO mice showed decreased behavioural responses to electroconvulsive shock (ECS) with shorter tonic seizures and faster recovery times than WT mice (Rodriguez de Turco, Tang et al. 2001). This behavioural response was paralleled by decreased ECS-induced phosphatidylinositol-4,5-bis phosphate (PIP_2) degradation and reduced long term potentiation (LTP) in

hippocampal perforant path-dentate gyrus neurons (Rodriguez de Turco, Tang, Topham, Sakane, Marcheselli, Chen, Taketomi, Prescott, and Bazan, 2001). The hippocampal dentate gyrus is an area of importance for learning, memory, and epileptogenesis. The observed resistance to seizures and attenuation of LTP in DGKε KO mice make DGKε an attractive target for studying epilepsy (Rodriguez de Turco, Tang, Topham, Sakane, Marcheselli, Chen, Taketomi, Prescott, and Bazan, 2001). Similarly, other studies using DGKε KO mice have linked DGKε to hippocampal plasticity-mediated kindling and epileptogenesis (Musto and Bazan, 2006). DGKε KO mice demonstrated a rapid behavioural recovery following brain stimulation and showed a lack of morphological changes in hippocampal glial cells, including the absence of hypertrophied cell bodies or elongated cell processes that were seen in WT mice (Musto and Bazan, 2006). Thus, DGKε appears to regulate seizure susceptibility and LTP via its involvement in PI signalling (Bazan, 2005; Musto and Bazan, 2006; Rodriguez de Turco, Tang, Topham, Sakane, Marcheselli, Chen, Taketomi, Prescott, and Bazan, 2001).

DGKε as a therapeutic target for Huntington's disease

Studies show that DGKε is an attractive target to attenuate Huntington's disease (HD) (Zhang, Li et al. 2012). Blocking DGKε in a mouse HD striatal cell model ($Hdh^{111Q/111Q}$) relieves mutant Huntingtin protein (Htt) mediated toxicity and reduces caspases 3 and 7 activities (Zhang, Li, Al-Ramahi, Cong, Held, Kim, Botas, Gibson, and Ellerby, 2012). Inhibition of DGKε with siRNAs or chemical inhibitors reduced proteolysis of mutant Htt and production of the toxic N-terminal Htt fragment that contributes to cell death in HD (Zhang, Li, Al-Ramahi, Cong, Held, Kim, Botas, Gibson,

and Ellerby, 2012). Mutant Htt appears to bind subsets of PIP_ns more strongly than the WT protein (Zhang, Li, Al-Ramahi, Cong, Held, Kim, Botas, Gibson, and Ellerby, 2012). *In vivo* analyses show that the level of DGKε in the striatum of transgenic HD mice is higher than in littermate controls, suggesting a specific role for DGKε in HD toxicity (Zhang, Li, Al-Ramahi, Cong, Held, Kim, Botas, Gibson, and Ellerby, 2012). Decreasing the levels of DGKε in a *Drosophila* HD model significantly reduces the toxic effects of mutant Htt, and strengthens the notion that Htt-DGKε interactions are relevant *in vivo* (Zhang, Li, Al-Ramahi, Cong, Held, Kim, Botas, Gibson, and Ellerby, 2012).

DGKε prevents cardiac hypertrophy and heart failure

Numerous studies implicate the $G_{\alpha q}$ protein-coupled receptor-signalling pathway leading to the phospholipase C-mediated hydrolysis of PIP_2 in the development of cardiac hypertrophy and heart failure (Hunter and Chien,1999; Takeishi, Jalili et al. 1999). The 20:4 DAG produced from the hydrolysis of PIP_2 is a potent activator of PKC. In turn, PKC activity has been associated to the development of cardiac hypertrophy and heart failure (Bowling, Walsh et al. 1999; Takeishi, Chu et al. 1998; Takeishi, Ping et al. 2000). In one study, overexpression of DGKε in porcine aortic endothelial cells specifically reduced the levels of 20:4 DAG while having a minimal effect on the levels of more saturated DAGs (Pettitt and Wakelam ,1999). Reducing 20:4 DAG levels decreases translocation of PKC_α and PKC_ε from the membrane to the cytosol; likely attenuating PKC mediated cardiac hypertrophy and progression to heart failure (Niizeki, Takeishi et al. 2008; Pettitt and Wakelam, 1999). Other studies using transgenic mice with cardiac-

specific over-expression of DGKε show higher survival rates compared to WT mice when chronic pressure overload is induced by phenylephrine infusion or transverse aortic constriction (Niizeki, Takeishi, Kitahara, Arimoto, Ishino, Bilim, Suzuki, Sasaki, Nakajima, Walsh, Goto, and Kubota, 2008). Phenylephrine and transverse aortic constriction induced accumulation of DAG, PKC translocation, induction of fetal genes, and upregulation of transient receptor potential channel-6 were all blocked in DGKε-transgenic mice (Niizeki, Takeishi, Kitahara, Arimoto, Ishino, Bilim, Suzuki, Sasaki, Nakajima, Walsh, Goto, and Kubota, 2008).

Mutations in the DGKε gene are linked to renal diseases

Studies reveal that DGKε is also implicated in maintaining renal function, since mutations in the enzyme have been associated with atypical hemolytic uremic syndrome as well as membranoproliferative-like glomerular microangiopathy (Lemaire, Fremeaux-Bacchi et al. 2013; Ozaltin, Li et al. 2013). The DGKε mutations resulting in disease phenotypes were primarily found in the catalytic domain, and resulted in increased DAG levels. DGKε typically attenuates DAG signalling, which is responsible for PKC activation and the promotion of thrombosis. Therefore, it is likely that the loss of DGKε function could result in a prothrombotic state and the observed disease phenotypes (Lemaire, Fremeaux-Bacchi, Schaefer, Choi, Tang, Le, Fakhouri, Taque, Nobili, Martinez, Ji, Overton, Mane, Nurnberg, Altmuller, Thiele, Morin, Deschenes, Baudouin, Llanas, Collard, Majid, Simkova, Nurnberg, Rioux-Leclerc, Moeckel, Gubler, Hwa, Loirat, and Lifton, 2013). It has recently been suggested that the mechanism of inducing

activation of kidney endothelial cells through the loss of DGKε is by increasing apoptosis and impairing endothelial cell proliferation and angiogenesis (Bruneau, Neel et al. 2015) or alternatively by a complement-dependent mechanism (Bruneau, Neel, Roumenina, Frimat, Laurent, Fremeaux-Bacchi, and Fakhouri, 2015).

VIII. Summary and Future Perspectives

The most hydrophobic segment of DGKε, comprised of residues 20 to 42, appears to have no role in binding the lipid substrate DAG or in the acyl chain specificity of substrate phosphorylation. Nevertheless, the sequence in this segment of DGKε is highly conserved among multicellular eucaryotes, with few if any conservative substitutions. We show that this segment is important for anchoring the protein to the membrane. Although it has no function in *in vitro* assays of catalytic activity, it likely has an important function in the context of the whole cell. This function could include regulating the activity of the enzyme depending on whether this segment forms a transmembrane helix or a re-entrant helix. *In silico* calculations suggest the possibility of such a conformational change (Decaffmeyer, Shulga, Dicu, Thomas, Truant, Topham, Brasseur, and Epand, 2008). This conformational switch would not likely be observed with the current *in vitro* assays of catalytic activity that are conducted in mixed micelles. However, we are currently developing a liposome-based assay for DGKε. In addition to effects on catalysis, the hydrophobic segment may also have a role, in the context of the whole cell, in protein-protein interactions or in translocation of DGKε between membranes. These functions

may be particularly important for DGKε since this enzyme catalyzes a step in the PI-cycle that has to segregate lipid substrates and products from other metabolic pathways. Membrane translocation is also important because steps in the PI-cycle take place both in the endoplasmic reticulum and in the plasma membrane. There is evidence for DGKε being present in both of these membranes.

The catalytic mechanism of DGKε is conserved from the bacterial enzyme, DgkB. However, all mammalian forms of DGK are much larger than DgkB; including the smallest isoform, DGKε. This allows the mammalian DGKs to evolve additional specific properties. In the case of DGKε, one of these properties is the specificity for substrates containing arachidonic acid. This specificity is not a result of the presence of the hydrophobic segment near the amino terminus of DGKε. We suggest that a pattern of amino acid residues similar to that found to be important for the recognition of arachidonic acid by lipoxygenases is responsible for this specificity. This suggests that, as with lipoxygenases, DGKε binds the hydrophobic arachidonoyl group in a channel of the protein outside of the bilayer. The importance of the acyl chain specificity of DGKε is to allow this enzyme to contribute to the enrichment of lipid intermediates of the PI-cycle with 1-stearoyl-2-arachidonoyl species (Epand, 2015). Mutations or deletions of DGKε are associated with several disease processes.

Reference List

Abe, T., Lu, X., Jiang, Y., Boccone, C.E., Qian, S., Vattem, K.M., Wek, R.C., and Walsh, J.P., 2003. Site-directed mutagenesis of the active site of diacylglycerol kinase alpha: calcium and phosphatidylserine stimulate enzyme activity via distinct mechanisms. **Biochem.J. 375**, 673-680.

Aveldano, M.I. and Bazan, N.G., 1975. Rapid production of diacylglycerols enriched in arachidonate and stearate during early brain ischemia. **J.Neurochem. 25**, 919-920.

Bazan, N.G., 2005. Lipid signaling in neural plasticity, brain repair, and neuroprotection. **Mol Neurobiol. 32**, 89-103.

Bazan, N.G., Morelli de Liberti, S.A., and Rodriguez de Turco, E.B., 1982. Arachidonic acid and arachidonoyl-diglycerols increase in rat cerebrum during bicuculline-induced status epilepticus. **Neurochem.Res. 7**, 839-843.

Bowling, N., Walsh, R.A., Song, G., Estridge, T., Sandusky, G.E., Fouts, R.L., Mintze, K., Pickard, T., Roden, R., Bristow, M.R., Sabbah, H.N., Mizrahi, J.L., Gromo, G., King, G.L., and Vlahos, C.J., 1999. Increased protein kinase C activity and expression of Ca2+-sensitive isoforms in the failing human heart. **Circulation 99**, 384-391.

Bruneau, S., Neel, M., Roumenina, L.T., Frimat, M., Laurent, L., Fremeaux-Bacchi, V., and Fakhouri, F., 2015. Loss of DGKe induces endothelial cell activation and death independently of complement activation. **Blood 125**, 1038-1046.

Buchan, D.W., Minneci, F., Nugent, T.C., Bryson, K., and Jones, D.T., 2013. Scalable web services for the PSIPRED Protein Analysis Workbench. **Nucleic Acids Res. 41**, W349-W357.

D'Souza, K. and Epand, R.M., 2012. Catalytic activity and acyl-chain selectivity of diacylglycerol kinase epsilon are modulated by residues in and near the lipoxygenase-like motif. **J.Mol Biol 416**, 619-628.

-----, 2014. Enrichment of phosphatidylinositols with specific acyl chains. **Biochim.Biophys.Acta 1838**, 1501-1508.

D'Souza, K., Kim, Y.J., Balla, T., and Epand, R.M., 2014. Distinct Properties of the Two Isoforms of CDP-Diacylglycerol Synthase. **Biochemistry 53**, 7358-7367.

Decaffmeyer, M., Shulga, Y.V., Dicu, A.O., Thomas, A., Truant, R., Topham, M.K., Brasseur, R., and Epand, R.M., 2008. Determination of the topology of the hydrophobic segment of mammalian diacylglycerol kinase epsilon in a cell membrane and its relationship to predictions from modeling. **J.Mol Biol 383**, 797-809.

Dicu, A.O., Topham, M.K., Ottaway, L., and Epand, R.M., 2007. Role of the hydrophobic segment of diacylglycerol kinase epsilon. **Biochemistry 46**, 6109-6117.

Epand, R.M., 2015. Enrichment of acyl chains in the lipids of the phosphatidylinositol cycle. **ASBMB Today 14**, 16-17.

Glukhov, E., Shulga, Y.V., Epand, R.F., Dicu, A.O., Topham, M.K., Deber, C.M., and Epand, R.M., 2007. Membrane interactions of the hydrophobic segment of diacylglycerol kinase epsilon. **Biochim.Biophys.Acta 1768**, 2549-2558.

Han, G.S., O'Hara, L., Siniossoglou, S., and Carman, G.M., 2008. Characterization of the Yeast DGK1-encoded CTP-dependent Diacylglycerol Kinase. **Journal of Biological Chemistry 283**, 20443-20453.

Horrocks, L.A. and Farooqui, A.A., 1994. NMDA receptor-stimulated release of arachidonic acid: mechanisms for the Bazan effect. *Cell Signal Transduction, Second Messengers, and Protein Phosphorylation in Health and Disease* Springer, U.S., pp. 113-128.

Hunter, J.J. and Chien, K.R., 1999. Signaling pathways for cardiac hypertrophy and failure. **N.Engl.J.Med. 341**, 1276-1283.

Jerga, A., Lu, Y.J., Schujman, G.E., de, M.D., and Rock, C.O., 2007. Identification of a soluble diacylglycerol kinase required for lipoteichoic acid production in *Bacillus subtilis*. **J.Biol Chem. 282**, 21738-21745.

Jones, D.T., 1999. Protein secondary structure prediction based on position-specific scoring matrices. **J.Mol Biol 292**, 195-202.

Kobayashi, N., Hozumi, Y., Ito, T., Hosoya, T., Kondo, H., and Goto, K., 2007. Differential subcellular targeting and activity-dependent subcellular localization of diacylglycerol kinase isozymes in transfected cells. **Eur.J.Cell Biol 86**, 433-444.

Lemaire, M., Fremeaux-Bacchi, V., Schaefer, F., Choi, M., Tang, W.H., Le, Q.M., Fakhouri, F., Taque, S., Nobili, F., Martinez, F., Ji, W., Overton, J.D., Mane, S.M., Nurnberg, G., Altmuller, J., Thiele, H., Morin, D., Deschenes, G., Baudouin, V., Llanas, B., Collard, L., Majid, M.A., Simkova, E., Nurnberg, P., Rioux-Leclerc, N., Moeckel, G.W., Gubler, M.C., Hwa, J., Loirat, C., and Lifton, R.P., 2013. Recessive mutations in DGKE cause atypical hemolytic-uremic syndrome. **Nat.Genet. 45**, 531-536.

Lukiw, W.J., Cui, J.G., Musto, A.E., Musto, B.C., and Bazan, N.G., 2005. Epileptogenesis in diacylglycerol kinase epsilon deficiency up-regulates COX-2 and tyrosine hydroxylase in hippocampus. **Biochem.Biophys.Res.Commun. 338**, 77-81.

Lung, M., Shulga, Y.V., Ivanova, P.T., Myers, D.S., Milne, S.B., Brown, H.A., Topham, M.K., and Epand, R.M., 2009. Diacylglycerol kinase epsilon is selective for both acyl chains of phosphatidic acid or diacylglycerol. **J.Biol.Chem. 284**, 31062-31073.

Matsui, H., Hozumi, Y., Tanaka, T., Okada, M., Nakano, T., Suzuki, Y., Iseki, K., Kakehata, S., Topham, M.K., and Goto, K., 2014. Role of the N-terminal hydrophobic residues of DGKepsilon in targeting the endoplasmic reticulum. **Biochim.Biophys.Acta 1841**, 1440-1450.

Miller, D.J., Jerga, A., Rock, C.O., and White, S.W., 2008. Analysis of the *Staphylococcus aureus* DgkB structure reveals a common catalytic mechanism for the soluble diacylglycerol kinases. **Structure. 16**, 1036-1046.

Milne, S.B., Ivanova, P.T., Armstrong, M.D., Myers, D.S., Lubarda, J., Shulga, Y.V., Topham, M.K., Brown, H.A., and Epand, R.M., 2008. Dramatic differences in the roles in lipid metabolism of two isoforms of diacylglycerol kinase. **Biochemistry 47**, 9372-9379.

Musto, A. and Bazan, N.G., 2006. Diacylglycerol kinase epsilon modulates rapid kindling epileptogenesis. **Epilepsia 47**, 267-276.

Nakano, T., Hozumi, Y., Goto, K., and Wakabayashi, I., 2009. Localization of diacylglycerol kinase epsilon on stress fibers in vascular smooth muscle cells. **Cell Tissue Res. 337**, 167-175.

Neau, D.B., Gilbert, N.C., Bartlett, S.G., Boeglin, W., Brash, A.R., and Newcomer, M.E., 2009. The 1.85 A structure of an 8R-lipoxygenase suggests a general model for lipoxygenase product specificity. **Biochemistry 48**, 7906-7915.

Niizeki, T., Takeishi, Y., Kitahara, T., Arimoto, T., Ishino, M., Bilim, O., Suzuki, S., Sasaki, T., Nakajima, O., Walsh, R.A., Goto, K., and Kubota, I., 2008. Diacylglycerol kinase-epsilon restores cardiac dysfunction under chronic pressure overload: a new specific regulator of Galpha(q) signaling cascade. **Am.J.Physiol Heart Circ.Physiol 295**, H245-H255.

Norholm, M.H., Shulga, Y.V., Aoki, S., Epand, R.M., and von Heijne, G., 2011. Flanking residues help determine whether a hydrophobic segment adopts a monotopic or bitopic topology in the endoplasmic reticulum membrane. **J.Biol Chem. 286**, 25284-25290.

Ozaltin, F., Li, B., Rauhauser, A., An, S.W., Soylemezoglu, O., Gonul, I.I., Taskiran, E.Z., Ibsirlioglu, T., Korkmaz, E., Bilginer, Y., Duzova, A., Ozen, S., Topaloglu, R., Besbas, N., Ashraf, S., Du, Y., Liang, C., Chen, P., Lu, D., Vadnagara, K., Arbuckle, S., Lewis, D., Wakeland, B., Quigg, R.J., Ransom, R.F., Wakeland, E.K., Topham, M.K., Bazan, N.G., Mohan, C., Hildebrandt, F., Bakkaloglu, A., Huang, C.L., and Attanasio, M., 2013. DGKE variants cause a glomerular microangiopathy that mimics membranoproliferative GN. **J.Am.Soc.Nephrol. 24**, 377-384.

Pettitt, T.R. and Wakelam, M.J., 1999. Diacylglycerol kinase epsilon, but not zeta, selectively removes polyunsaturated diacylglycerol, inducing altered protein kinase C distribution in vivo. **J.Biol Chem. 274**, 36181-36186.

Prodeus, A., Berno, B., Topham, M.K., and Epand, R.M., 2013. The basis of the substrate specificity of the epsilon isoform of human diacylglycerol kinase is not a consequence of competing hydrolysis of ATP. **Chem.Phys.Lipids 166**, 26-30.

Rodriguez de Turco, E.B., Tang, W., Topham, M.K., Sakane, F., Marcheselli, V.L., Chen, C., Taketomi, A., Prescott, S.M., and Bazan, N.G., 2001. Diacylglycerol kinase epsilon regulates seizure susceptibility and long-term potentiation through arachidonoyl- inositol lipid signaling. **Proc.Natl.Acad.Sci.U.S.A 98**, 4740-4745.

Roy, A., Kucukural, A., and Zhang, Y., 2010. I-TASSER: a unified platform for automated protein structure and function prediction. **Nat Protoc. 5**, 725-738.

Shulga, Y.V., Myers, D.S., Ivanova, P.T., Milne, S.B., Brown, H.A., Topham, M.K., and Epand, R.M., 2010. Molecular species of phosphatidylinositol-cycle intermediates in the endoplasmic reticulum and plasma membrane. **Biochemistry 49**, 312-317.

Shulga, Y.V., Topham, M.K., and Epand, R.M., 2011a. Regulation and functions of diacylglycerol kinases. **Chem.Rev. 111**, 6186-6208.

-----, 2011b. Study of arachidonoyl specificity in two enzymes of the PI cycle. **J.Mol.Biol. 409**, 101-112.

Soding, J., 2005. Protein homology detection by HMM-HMM comparison. **Bioinformatics. 21**, 951-960.

Sun, G.Y., Xu, J., Jensen, M.D., and Simonyi, A., 2004. Phospholipase A2 in the central nervous system: implications for neurodegenerative diseases. **J.Lipid Res. 45**, 205-213.

Takeishi, Y., Chu, G., Kirkpatrick, D.M., Li, Z., Wakasaki, H., Kranias, E.G., King, G.L., and Walsh, R.A., 1998. In vivo phosphorylation of cardiac troponin I by protein kinase Cbeta2 decreases cardiomyocyte calcium responsiveness and contractility in transgenic mouse hearts. **J.Clin Invest 102**, 72-78.

Takeishi, Y., Jalili, T., Ball, N.A., and Walsh, R.A., 1999. Responses of cardiac protein kinase C isoforms to distinct pathological stimuli are differentially regulated. **Circ.Res. 85**, 264-271.

Takeishi, Y., Ping, P., Bolli, R., Kirkpatrick, D.L., Hoit, B.D., and Walsh, R.A., 2000. Transgenic overexpression of constitutively active protein kinase C epsilon causes concentric cardiac hypertrophy. **Circ.Res. 86**, 1218-1223.

Ullrich, S.J., Hellmich, U.A., Ullrich, S., and Glaubitz, C., 2011. Interfacial enzyme kinetics of a membrane bound kinase analyzed by real-time MAS-NMR. **Nat Chem.Biol 7**, 263-270.

Van Horn, W.D., Kim, H.J., Ellis, C.D., Hadziselimovic, A., Sulistijo, E.S., Karra, M.D., Tian, C., Sonnichsen, F.D., and Sanders, C.R., 2009. Solution nuclear magnetic resonance structure of membrane-integral diacylglycerol kinase. **Science 324**, 1726-1729.

Van Horn, W.D. and Sanders, C.R., 2012. Prokaryotic diacylglycerol kinase and undecaprenol kinase. **Annu.Rev Biophys. 41**, 81-101.

Yang, J., Yan, R., Roy, A., Xu, D., Poisson, J., and Zhang, Y., 2015. The I-TASSER Suite: protein structure and function prediction. **Nature Methods 12**, 7-8.

Zhang, N., Li, B., Al-Ramahi, I., Cong, X., Held, J.M., Kim, E., Botas, J., Gibson, B.W., and Ellerby, L.M., 2012. Inhibition of lipid signaling enzyme diacylglycerol kinase epsilon attenuates mutant huntingtin toxicity. **J.Biol Chem. 287**, 21204-21213.

Zhang, Y., 2008. I-TASSER server for protein 3D structure prediction. **BMC Bioinformatics. 9**, 40.

Acknowledgements:

This work was supported by the Natural Sciences and Engineering Council of Canada, grant 9848 (to RME). We are also grateful to Christopher M. Yip and Amy Won for help with the AFM study and to Alba Guarné for helpful discussions regarding protein modeling.

Figure Legends

Figure 1. Using the Web based program for predicting transmembrane helices, TMHMM (http://www.cbs.dtu.dk/services/TMHMM/), a segment near the amino terminus is the only segment predicted to be transmembrane.

Figure 2. *Comparison of sequences around the active sites of DGKε and DgkA.* The sequences were aligned using the NCBI protein Basic Local Alignment Search Tool (BLAST). Blue rectangles represent alpha helices, and purple arrows represent beta strands.

Figure 3. *I-TASSER prediction of human DGKε tertiary structure.* The sequence for human DGKε was analyzed with the I-TASSER hierarchical protein structure modeling approach. Five tertiary structure predictions were generated, and the figure includes one of the predictions with a C value of -2.33, an estimated TM-score of 0.54±0.15 and an estimated RMSD score of 10.9±4.6Å. (A) Human DGKε tertiary structure prediction by I-TASSER showing the lipoxygenase motif in orange, the *GGDG* sequence (p-motif) of the active site domain in red and the membrane associating alpha helix in purple. The image was created using PyMOL. (B) The confidence of the I-TASSER prediction is presented in Ångströms, and the secondary structure prediction is seen at the bottom (red is alpha helices and green represents beta strands).

Figure 4. *Alignment of Bacterial DgkB and Human DGKε Sequences*. The sequences for residues 274-373 of human DGKε and residues 62-147 of *Staphylococcus aureus* DgkB were aligned using the NCBI protein Basic Local Alignment Search Tool (BLAST). The determined (DgkB) and PSIPRED predicted DGKε secondary structures were superimposed on their respective sequences (blue rectangles represent alpha helices, and purple arrows represent beta strands).

Figure 5. *Human DGKε I-TASSER tertiary structure prediction and Bacterial DgkB crystal structure alignment.* One of the five I-TASSER tertiary structure predictions for residues 213-373 of Human DGKε was aligned with residues 1-160 of the known crystal structure for DgkB. (A) Residues 213-373 of the Human DGKε tertiary structure prediction are highlighted in red, and the remainder of the structure is seen in blue. (B) Residues 1-160 of the bacterial DgkB tertiary structure are highlighted in red, while the remainder of the structure is seen in purple. (C) Residues 213-373 of Human DGKε (blue) was aligned with residues 1-160 of DgkB (purple). Similarities between the tertiary structures are observed in this region.

Figure 6. *Hydrophobicity of Human DGKε.* The hydrophobic and hydrophilic residues in the I-TASSER tertiary structure prediction of Human DGKε are highlighted. (A) The catalytic site and its five amphipathic alpha helices are highlighted; the blue residues are hydrophilic and the yellow residues are hydrophobic. (B) The hydrophobic and hydrophilic residues are highlighted on the lipoxygenase motif, the catalytic site and the

membrane associating alpha helix. In these specific areas, hydrophilic residues are blue, and hydrophobic residues are yellow. The remainder of the molecule is grey.

Figure 7. *Charge of Human DGKε I-TASSER tertiary structure prediction.* The positive and negative residues of human DGKε are highlighted in the active site. Blue residues are negative and yellow residues are positive, the remainder of the active site residues are red.

Figures:

Figure 1

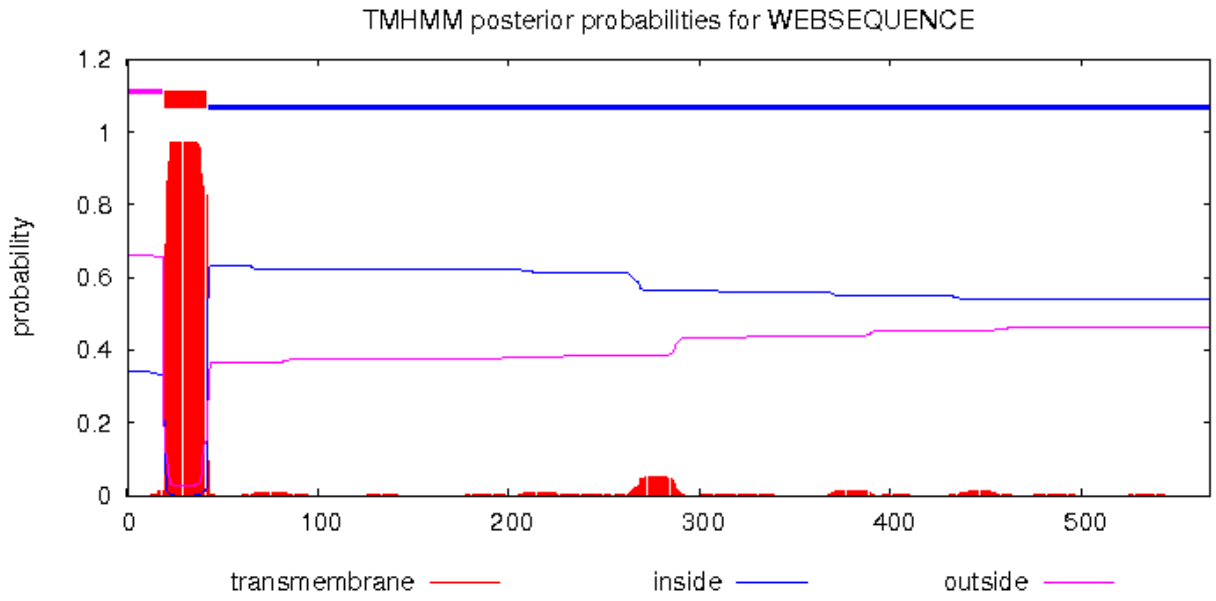

Figure 2


DGKε 271 SARVLVCGGDGTVGWVL 287
SA VL+ D + W +
DgkA 100 SAAVLIAIIDAVITWCI 116

Figure 3

A

B

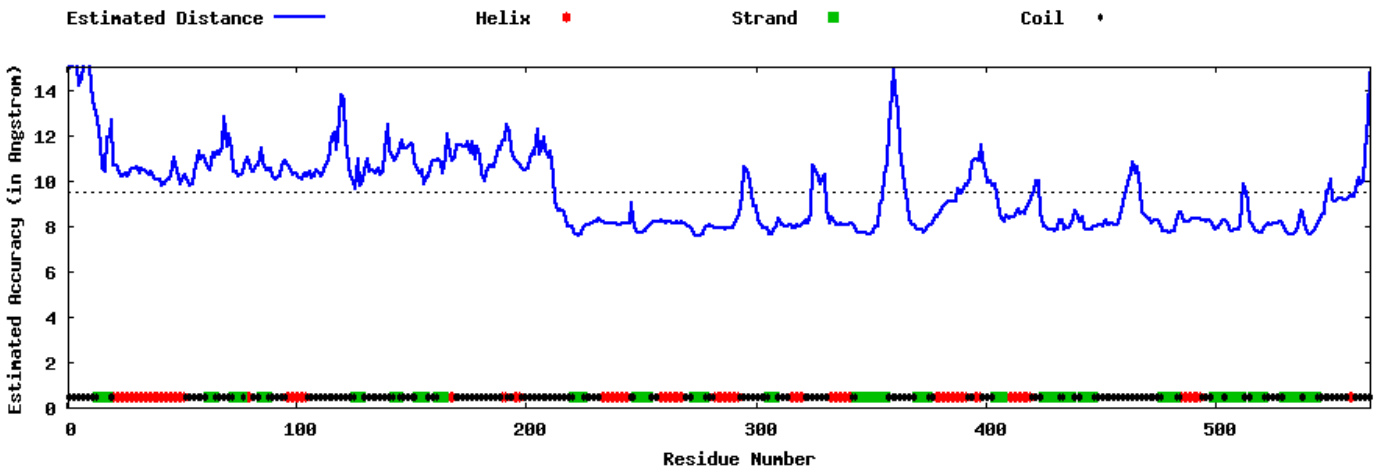
Estimated Distance
Helix
Strand
Coil
Estimated Accuracy (in Angstron)
0
2
4
6
8
10
12
14
0
100
200
300
400
500
Residue Number

Figure 4

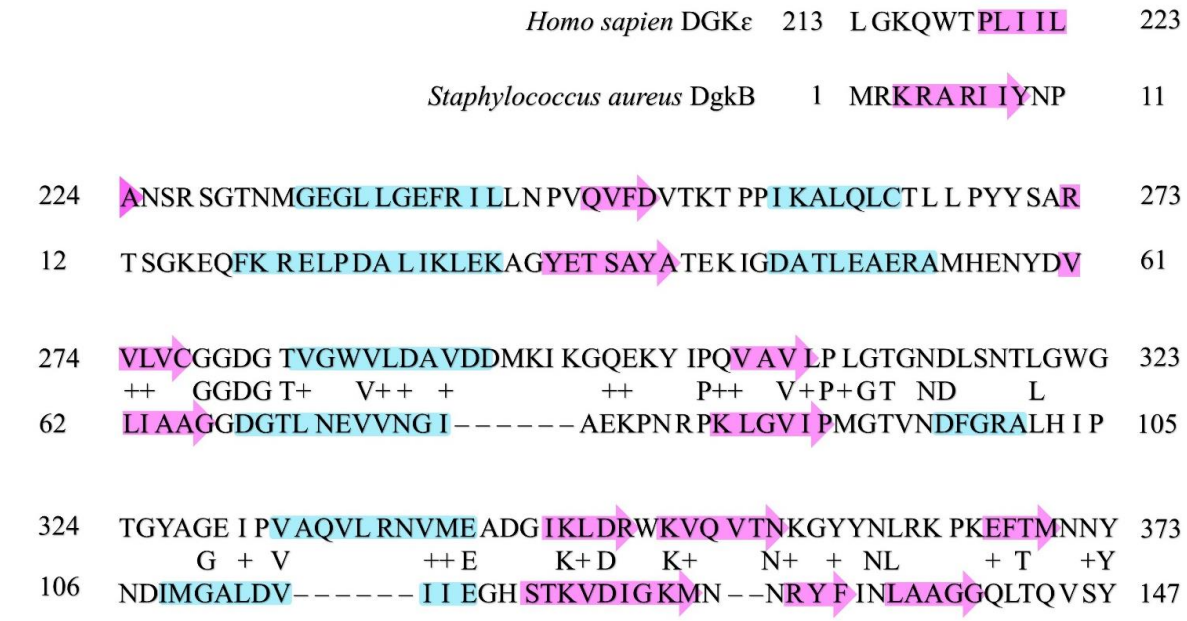
Homo sapien DGKε 213 L GKQWT PL I IL 223
Staphylococcus aureus DgkB 1 MRK RA RI IYNP 11
224 ANSR SGTNMGEGL LGEFR I LL N PVQVFDVTKT PP I KALQLCT L L PYY SAR 273
12 T SGKEQFK R ELP DA L IKLEK AGYET SAY A TE K IGDA TL EAERA MHENYDV 61
274 VLVCGGDG TVGWVLDA VDDMKI KGQEKY IPQV A V LP LGTGNDLSNTLGWG 323
++ GGDG T+ V+ + + ++ P++ V+P+GT ND L
62 LI AAGGDGTL NEVVNG I – – – – – – AEKPN R PK LGV I PMGTVNDFGRALH I P 105
324 TGYAGE I PV AQVL RNVME ADG IKL DRWKVQ VTNKGYYNLRK PKEFTMNNY 373
G + V ++ E K+ D K+ N+ + NL + T +Y
106 NDIMGALDV – – – – – – I I EGH STKVDIG KMN – – NR Y F INLAAGGQLTQ V SY 147

Figure 5

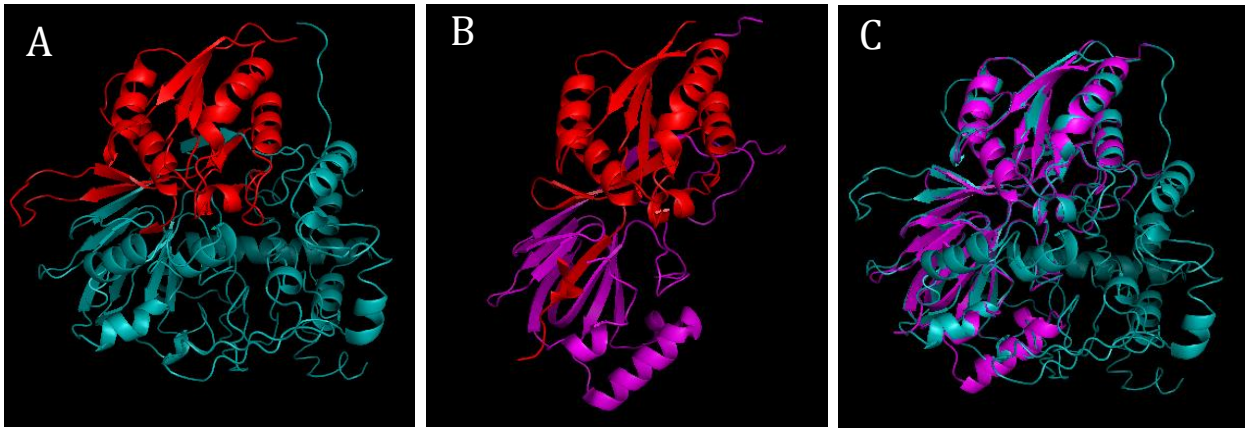

Figure 6

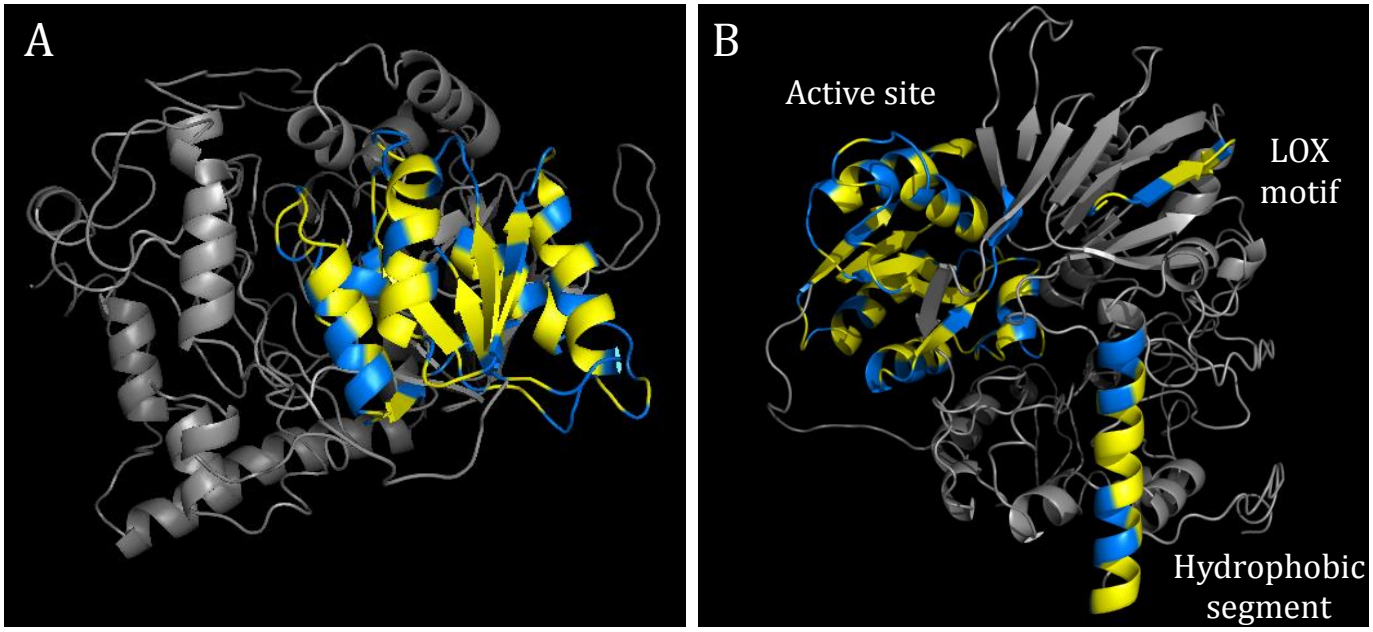

Figure 7

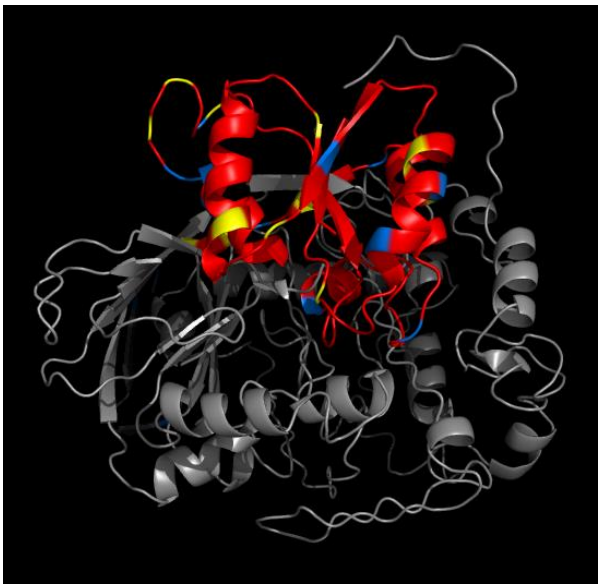

CHAPTER 2: Introduction

Expression, Purification and Properties of a Human Arachidonoyl-Specific Isoform of Diacylglycerol Kinase

William Jennings, Sejal Doshi, Prasanta Kumar Hota, Aaron Prodeus, Stephanie Black and Richard M. Epand

This paper describes the purification of DGKε and a truncated version of the protein lacking the first forty amino acid residues (DGKε Δ40). We show that both proteins can be expressed in Sf21 cells and can be purified to near homogeneity using nickel affinity chromatography. We provide a partial characterization of both proteins as well as a comparison of their stability in the purified form. My contribution to this paper was performing all of the experiments with the assistance of Sejal Doshi and Stephanie Black (Figures 1-11, Table 1 and supplementary figures 1-2), writing the manuscript, and editing the manuscript with the help of Richard Epand. Aaron Prodeus and Prasanta Hota performed initial studies developing the Sf21 expression system and the DGKε purification protocol respectively.

---

[1] Jennings, W., Doshi, S., Hota, P., Prodeus, A., & Epand, R. M. (2015). Expression, Purification and Properties of a Human Arachidonoyl-Specific Isoform of Diacylglycerol Kinase. (Being submitted).

Expression, Purification and Properties of a Human Arachidonoyl-Specific Isoform of Diacylglycerol Kinase[†]

William Jennings, Sejal Doshi, Prasanta Kumar Hota, Aaron Prodeus, Stephanie Black, and Richard M. Epand

Department of Biochemistry and Biomedical Sciences, McMaster University, 1280 Main Street West, Hamilton, Ontario L8S 4K1, CANADA.

Address correspondence to: Richard M. Epand, Department of Biochemistry and Biomedical Sciences, McMaster University, 1280 Main Street West, Hamilton, Ontario L8S 4K1, CANADA;

Tel. 905 525-9140 Ext: 22073; Fax 905 521-1397; E-mail: epand@mcmaster.ca

RUNNING HEAD: Diacylglycerol Kinase Epsilon

[†]This work was supported by the Natural Sciences and Engineering Council of Canada, grant 9848 (to RME).

[1]Abbreviations: BEVS, Baculovirus Expression Vector System; CD, Circular Dichroism; DAG, 1,2-diacylglycerol; DGK, diacylglycerol kinase; DGKεΔ40**,** truncated Diacylglycerol Kinase Epsilon lacking 40 amino acid residues at N-terminus; DLG, 1,2-dilinoleoyl-*sn*-glycerol; DOPC, 1,2-Dioleoyl-sn-glycero-3-phosphocholine; EV, empty vector; DGKε-$His_{(6)}$, Diacylglycerol Kinase Epsilon containing a hexahistidine epitope tag on the C-terminus; FBS, fetal bovine serum; MEF, mouse embryonic fibroblast; Ni-NTA, nickel nitrilotriacetic acid; PBS, phosphate buffered saline; PCR, polymerase chain reaction; SAG,1-Stearoyl-2-arachidonoyl-*sn*-glycerol; SLG, 1-Stearoyl-2-linoleoyl-*sn*-glycerol; SUV**,** small unilamellar vesicle; TBST, Tris buffered saline with Tween 20.

ABSTRACT

Diacylglycerol kinase epsilon (DGKε) catalyzes the phosphorylation of diacylglycerol producing phosphatidic acid. DGKε demonstrates specificity for the acyl chains of its diacylglycerol substrate and consequently is an integral regulator of phosphatidylinositol signaling. Dysregulation of DGKε perturbs lipid signaling and biosynthesis, which has been linked to atypical hemolytic uremic syndrome, and may also play a role in epilepsy, Huntington's disease and heart disease. Little is known about the molecular properties of DGKε because it has never been purified. We expressed human DGKε and a truncated version with the first 40 residues deleted (DGKεΔ40) and purified both proteins to near homogeneity using Nickel-affinity chromatography. Kinase activity measurements showed that both purified constructs retained their specificity for the acyl chains of DAG with an activity comparable to that of N-terminally FLAG epitope tagged forms of these proteins expressed in Cos-7 cells. Both constructs demonstrated kinase activity loss upon storage, particularly upon freeze thawing, which we were able to minimize with glycerol. Circular dichroism revealed that DGKε contains significant amounts of α-helical and β-structure. Both DGKε and DGKεΔ40 exhibit a biphasic transition from the folded to unfolded states upon heating. The loss of secondary structure was irreversible for both constructs with relatively little effect of added dioleoyl-phosphatidylcholine. 50% glycerol stabilized both constructs and facilitated refolding of their secondary structure. This is the first successful purification and characterization of DGKε's enzymatic and conformational properties. The purification of DGKε finally

allows for a detailed analysis of this unique enzyme and will improve our understanding of DGKε-related diseases.

INTRODUCTION

There are 10 isoforms of diacylglycerol kinase (DGK)[1] identified to date, as well as gene-splice variants of these isoforms, present in mammals. This family of proteins has a wide range of roles in signal transduction (*1*). Among all of these forms of DGK, only the epsilon isoform (DGKε) has been shown to exhibit specificity for molecular species of diacylglycerol (DAG) having particular acyl chains. DGKε favors DAG substrates with an arachidonoyl moiety at the sn-2 position (*2*) and a stearoyl group at the sn-1 position (*3*). There is evidence that DGKε acts through inositol lipid signaling (*4*) and it has been shown that this isoform of DGK affects both the arachidonoyl content of phosphatidylinositol lipids (*5*) as well as the stearoyl content (*3*). DGKε has also been associated with several important physiological functions and disease processes. DGKε knockout mice are resistant to electroconvulsive shock and kindling; conditions linked to deficiencies in long-term neuronal potentiation (*4*). The involvement of DGKε in kindling and long-term potentiation makes it an attractive target for epilepsy. DGKε also appears to have a role in the attenuation of Huntington's disease. Blocking DAG-activated transient receptor potential channels blocks neurotoxicity found in Huntington's disease (*6*). Recent work has also identified roles for DGKε in renal function; mutations in the DGKε gene were identified in membranoproliferative-like glomerular microangiopathy and atypical hemolytic-uremic syndrome (*7;8*). Studies using transgenic mice with cardiac-specific over-expression of DGKε have shown higher levels of survival compared to wild type mice under conditions of chronic pressure overload by controlling cellular DAG levels and transient receptor potential channel-6 expression (*9*). It is also suggested

that DGKε may be a novel therapeutic target to prevent cardiac hypertrophy and progression to heart failure (*9*). Given the unique properties of DGKε and its association with many diseases, its purification marks a tremendous advancement towards a better understanding of its structure and function as well as increases the likelihood of developing therapies for DGKε related pathologies.

A practical challenge with studying the diacylglycerol kinase family of enzymes and the related disease states arises from the difficulty in distinguishing the individual functions of each isoform. The absence of isoform specific inhibitors is one of the reasons that the functions of the individual isoforms have not yet been fully clarified. The purification of DGKε is an essential step towards achieving a crystal structure of this enzyme. The crystal structure of DGKε would be invaluable in aiding the design of a specific inhibitor. It is worth mentioning that various techniques, such as knock-out models in mice have provided a basic understanding of the different functions these isoforms possess in distinct signaling pathways (*1*). While all of the isoforms catalyze the same reaction, they serve a range of different cellular functions (*1*). For instance, DGKα and DGKζ are important for immune function by regulating Ras signaling in white blood cells. In the heart, DGKε mediates the $G\alpha_q$ protein-coupled receptor signal transduction pathway that leads to cardiac hypertrophy and heart failure (*9*). Commercially available DGK inhibitors lack true specificity for any particular isoform. Recently, a novel DGKα inhibitor was discovered using a high-throughput chemical screen of over 9600 chemical compounds (*10*). Despite being a remarkable improvement over all of the other inhibitors of DGK, the DGKα inhibitor still decreased the activity of the other nine isoforms by

roughly 25% (*10*). Regardless, this breakthrough will facilitate a better understanding of the particular function of DGKα within the cell. Additionally, the inhibitor possesses therapeutic value: it has been shown to attenuate cancer cell proliferation and simultaneously enhance immune responses and anticancer immunity (*10*). A specific inhibitor for the only isoform that displays acyl chain specificity for diacylglycerol would be invaluable for elucidating DGKε's role in lipid biosynthesis and various disease states, including atypical hemolytic uremic syndrome and epilepsy. However, some of the molecular features of the enzyme are not well established because the enzyme has never been isolated in purified form, except for one report on the purification of this protein from bovine testes (*11*). However, that protein had a lower mass than the full length mammalian DGKε and also had lost the acyl chain specific inhibition induced by phosphatidic acid (*3*).

The difficulties with purifying DGKε are that the protein is not very water soluble and it has a high affinity for membranes (*12*). Both of these properties have made the task of generating a homogenous and monodisperse sample of DGKε particularly challenging. In addition, the purified enzyme was found to be unstable when stored, even in the frozen state. Nevertheless, we have been able to isolate a C-terminally $His_{(6)}$-tag labeled form of full length DGKε and have also increased the stability of the protein by expressing an N-terminally truncated form, lacking the first 40 N-terminal residues, including the hydrophobic segment, residues 20-40. The most hydrophobic segment of DGKε comprises residues 20-42 and is predicted to form a transmembrane helix according to most predictive programs, including **TMHMM Server, v.2.0** (*13;14*). In addition to not

altering the enzymatic activity of DGKε, deleting this hydrophobic segment has been reported to not alter the acyl chain specificity toward arachidonoyl-containing DAG substrates (*3*). Interestingly, experimental evidence exists for both this hydrophobic segment forming a transmembrane helix (*15*) and a re-entrant helix (*16*). Mutating a single key residue in the middle of this helix (P32A) was shown to convert the helix from a re-entrant helix to a transmembrane helix and increase the enzyme's affinity for membranes (*16*). It is possible that, as predicted by *in silico calculations {Decaffmeyer, 2008 69 /id}* both conformations have similar stabilities and are readily interconvertible. The equilibrium between the two conformations may be affected by factors such as the composition and physical properties of the surrounding lipid in the bilayer, interactions with other proteins, or the binding of ATP or lipid. Evidence exists for the hydrophobic segment being critical for the targeting of DGKε to the ER membrane (17). This segment of DGKε plays a critical role in membrane insertion as well as enzyme localization and yet has a seemingly negligible effect on enzymatic activity (at least in a detergent-phospholipid mixed micelle system). There is an initial report on the lack of ATPase activity of the purified full length form of DGKε (*18*). In the present manuscript we describe the purification procedure. In addition, having for the first time a purified form of DGKε, it has allowed us to measure some of the enzymatic and molecular properties of DGKε and DGKε Δ40.

EXPERIMENTAL PROCEDURES

Cloning and construct preparation*:* To create a DGKε-$His_{(6)}$ and DGKεΔ40-$His_{(6)}$ construct in a pFastBac-CT-TOPO vector (Invitrogen) (pFastBac-CT-TOPO-DGKε-$His_{(6)}$ and pFastBac-CT-TOPO-DGKεΔ40-$His_{(6)}$), polymerase chain reaction (PCR) was used to amplify a DGKε product from a full-length cDNA template of human DGKε. The following primers were used: forward, 5'-ATGGAAGCGGAGAGGCGG-3'; reverse, 5'TTCAGTCGCCTTTATATCTTCTTG-3'. The following forward primer was used to prepare the pFastBac-CT-TOPO-DGKεΔ40-$His_{(6)}$ construct: 5'-ATGAGCCTCCAGCGGTCGCGC-3'(Mobix Lab, McMaster/Integrated DNA Technologies). PCR was conducted using Pfx DNA polymerase (Invitrogen) to get the blunt end PCR insert by following the manufacturer's recommendations. The product was separated on a 1% agarose gel, excised, and gel purified using a GeneJET Gel Extraction Kit (Thermo Scientific). The purified DNA construct was cloned into a pFastBac-CT-TOPO cloning vector (Invitrogen) and amplified in DH10Bac E. *coli* (Invitrogen). Samples were purified from DH10Bac E. *coli* using the Hipure linked DNA purification kit (Invitrogen). This vector was used to over express DGKε-$His_{(6)}$ and DGKεΔ40-$His_{(6)}$ protein products in Sf21 insect cells.

Insect cell expression: Sf21 cells (Invitrogen) were maintained in 1x Grace's insect cell media (Gibco) supplemented with 3.30 g/L lactalbumin hydrosylate (Sigma), 1x yeastolate ultrafiltrate (Invitrogen), 10% FBS (Gibco), 100 μg/mLPencilin-Streptomycin (Gibco), and 0.35 g/L sodium bicarbonate (Sigma). Cells were grown at 27°C and split at

confluency. To overexpress DGKε-$His_{(6)}$ and DGKεΔ40-$His_{(6)}$, $1x10^7$ cells were infected with recombinant baculovirus for 72 hours, before being scraped into PBS pH 7.4, centrifuged at 1000g for 10 minutes at 4°C, and stored at -80°C.

Cell lysate preparation: Frozen insect pellets overexpressing fusions were thawed and resuspended in cell lysis buffer (1x Tractor cell lysis buffer (Clontech) 500 µL/ T175 flask cell pellet, 2.5 mM sodium pyrophosphate, 1 mM β-glycerophosphate, 1 mM activated sodium orthovanadate, with 1:1000 dilution of Roche protease inhibitor cocktail tablet). Cells were allowed to lyse on ice for 15 minutes, followed by sonication for 5 minutes. The lysate was centrifuged at 100,000g for 60 minutes at 4°C in a Sorvall ultracentrifuge (RC-M120). These enriched supernatants were analyzed for recombinant DGKε expression and activity. Enriched lysates containing DGKε-$His_{(6)}$ and DGKεΔ40-$His_{(6)}$ from baculovirus infected Sf21 cells were treated with 20% glycerol and 0.05% β-mercaptoethanol for added stability before being purified as described below.

His tag DGKε purification using Ni NTA resin: 10 mL purification columns were prepared with approximately a 1:5 ratio (v/v) of Ni-NTA resin (Qiagen) to lysate and used to purify over-expressed DGKε-$His_{(6)}$ and DGKεΔ40-$His_{(6)}$ from Sf21 insect cells according to the manufacturer's instructions. Briefly, columns containing Ni-NTA resin were washed twice with double distilled H_2O by re-suspending the resin. Columns were then washed twice with equilibration buffer (50mM Sodium Phosphate, 300 mM Sodium Chloride, 10 mM Imidazole, 20% glycerol, 0.05% β-mercaptoethanol, pH7.4) by re-

suspension. Cell lysates (after centrifugation at 100,000g, 60 min, 4°C) were loaded into the washed and equilibrated columns and incubated at 4°C on a rocker for 1-2 hours. The flow through was removed and the resin was washed three times with wash buffer (50 mM Sodium Phosphate, 300 mM SodiumChloride, 20 mM Imidazole, 20% glycerol, 0.05% β-mercaptoethanol, pH7.4) for 20 minutes each at 4°C on a shaker. The bound protein was eluted with 2mL of elution buffer (50 mM Sodium phosphate, 300 mM Sodium Chloride, 100 mM Imidazole, 20% glycerol, 0.05% β-mercaptoethanol, pH 7.4) followed by a second 2 mL elution (50 mM Sodium phosphate, 300 mM Sodium Chloride, 200 mM Imidazole, 20% glycerol, 0.05% β-mercaptoethanol, pH 7.4). The elutions were performed for approximately one and two hours respectively on a shaker at 4°C. Protein concentration was measured with a Bradford Assay according to the manufacturer's protocol (BioRad). Note: immediately before use, β-mercaptoethanol and detergent were added to each buffer; 0.05% Tween 20 was used for all CD experiments.

Immunoblotting: Cell lysates were incubated with an equal volume of 2X Laemmli Sample Buffer at 70°C for 30 minutes, and loaded onto a 7.5% precast mini PROTEAN TGX gel (BioRad), and run at 120V. Proteins were transferred onto a polyvinylidene difluoride membrane (BioRad) and incubated in blocking solution composed of Tris-buffered saline, pH7.4, 0.1% Tween-20 (TBST) with 5% fat free skim milk powder for one hour. Membranes were then incubated overnight at 4°C with a 1:2000 dilution of mouse anti-$His_{(6)}$ antibody (GenScript). After washing in blocking buffer, membranes

were further incubated with horseradish peroxidise-conjugated goat anti-mouse antibody (GenScript) in a 1:2000 dilution for 1 hour. After washing in TBST buffer, antibody complexes were visualized with freshly prepared ECL solution (100 mM Tris pH 8.8, 1.25 mM luminol dissolved in DMSO, 2 mM 4-iodophenylboronic acid dissolved in DMSO, 0.016% H_2O_2 added last right before use).

Mixed micelle activity assay: A mixed micelle activity assay was used to measure DGKε activity from insect cell expression systems. This assay was adapted from those previously described (*9*). Lipid films composed of 8% (mol %) substrate (SAG or DLG) and 92% (mol %) phospholipid [e.g. 1,2- dioleoyl-*sn*-glycero-3-phosphocholine (DOPC)] (Avanti Polar Lipids), were hydrated in 4X assay buffer (200 mM MOPS pH 7.4, 400 mM NaCl, 20 mM $MgCl_2$, 4 mM EGTA pH 8.0, 60 mM Triton X-100, 1mM DTT), and vortexed for 2 minutes to create mixed micelles. The final concentration of the DAG substrate used per reaction was ~0.4 mM. If the mixed micelle solution was not clear, the solution was sonicated. The reaction mixture contained: 50 µL of 4X assay buffer/micelles, 20 µL cell lysates or purified protein solubilized in 2% IGEPAL, (protein volumes were adjusted to stay within the linear range of the assay and the volume was compensated for with elution buffer to ensure 20 µL was added to each reaction, 100 nmol (20 µL) [γ-^{32}P]-ATP (50µCi/mL) (Perkin Elmer Life Science), and 110 µL ddH_2O. The reaction was allowed to proceed for 10 minutes, before 2 mL of stop solution was added (1:1 $CHCl_3/CH_3OH$, 0.25mg/mL dihexadecyl$_{phosphate}$). The organic layer was washed 3 times with 2mL of wash solution (7:1 ddH_2O/CH_3OH, 1%

$HClO_4$, 0.1M H_3PO_4). To measure radioactive incorporation of ^{32}P into the organic-soluble phase, 400 µL of the organic phase was measured using a liquid scintillation counter (Beckman Coulter). We confirmed that the assay was linear with respect to protein amount and time. All samples were run in triplicate, and data is presented as means ± SEM. The purification protocol mentioned above for purifying DGKε-$His_{(6)}$ and DGKεΔ40-$His_{(6)}$ was performed on lysates prepared from Sf21 cells infected with mock DNA. The activity measured for the preparations purified from mock infected Sf21 cell lysates were subtracted from the activity of purified DGKε-$His_{(6)}$ and DGKεΔ40-$His_{(6)}$ samples to account for any lipid kinase activity arising from contaminating proteins. The activity values for the mock infected controls were obtained for each kinase activity experiment and were always significantly lower than the values from samples prepared from Sf21 cells infected with DGKε-$His_{(6)}$ or DGKεΔ40-$His_{(6)}$.

Calculation of DGKε-$His_{(6)}$ and DGKεΔ40-$His_{(6)}$ activity: To calculate the activity of purified DGKε-$His_{(6)}$ and DGKεΔ40-$His_{(6)}$, enzyme amounts were quantified using immunoblot analysis and densitometry using either a $His_{(6)}$ Molecular weight marker/standard (Qiagen) or a recombinant human N-terminal $His_{(6)}$ tagged lysophosphatidylcholine acyltransferase standard (BioVendor).

Circular dichroism spectroscopy: Ni-NTA purified DGKε-$His_{(6)}$ and DGKεΔ40-$His_{(6)}$ solubilized in 0.05% Tween 20 were dialyzed in PBS buffer (pH 6) with Slide-A-Lyzer Dialysis Cassettes (Thermo Scientific) according to the manufacturer's recommendations

to remove imidazole and excess salt. Circular dichroism (CD) spectroscopy was performed with an AVIV Circular Dichroism Model 410 spectrometer. The wavelength scan spectra from 260 to 196 nm in 1 nm intervals were recorded in a thermostated 1 mm path length quartz cuvette maintained at 25°C. CD spectra were measured in both the presence and absence of small unilamellar vesicles (SUVs) composed of DOPC at a lipid: protein molar ratio of 50:1. Three repeat scans were recorded using an averaging time of 5 seconds and1 nm bandwidth. Temperature scans of the ellipticity at 222nm were recorded from 20°C to 100°C followed by a cooling scan back to 20°C. Data was collected in mdeg and converted to mean residue ellipticity (degrees cm^2/dmol). Data was plotted using OrginPro 8 software and smoothed with the Adjacent-Averaging method. Wavelength scans were analyzed to determine secondary structure using the CONTINLL, SELCON3, and CDSSTR predictive algorithms with CDPro software. The output from CONTINLL, SELCON3 and CDSSTR were all in good agreement so the values obtained from each prediction were averaged.

Dynamic light scattering: Purified samples of DGKε-$His_{(6)}$ were assessed with dynamic light scattering using a Zetasizer Nano S (Malvern Instruments). Purified proteins (~20µM) were measured on 12 µL quartz cells at 4°C. Size distribution of the samples was calculated based on the correlation function provided by the Zetasizer software. Using Mie theory, the intensity- based distribution was transformed into a volume distribution to consider the relative proportion of potential multiple components in the sample.

RESULTS

Expression and purification of DGKε-His$_{(6)}$ and DGKε Δ40-His$_{(6)}$. DGK***ε***-His$_{(6)}$ and DGK***ε***Δ40-His$_{(6)}$ were expressed using the BEVS in Sf21 insect cells. Both constructs expressed well (approximately 0.95 mg of purified DGK***ε***-His$_{(6)}$ and 0.98 mg DGK***ε***Δ40-His$_{(6)}$ were extracted from 4 T175 flasks of Sf21 cells). An immunoblot performed on Ni-NTA purified DGK***ε***Δ40-His$_{(6)}$ shows an intense band around the expected 64 kDa and confirms successful expression (Figure 1). Immunoblots for DGK***ε***-His$_{(6)}$ looked very similar (not shown). An intense 64 kDa DGK***ε***-His$_{(6)}$ band was detected in the lysate (lane 1), and a considerably less intense band was detected in the flow through (lane 2). The wash fractions (lanes 3, 4 and 5) do not have any intense protein bands. To reduce the exposure of purified protein to imidazole, we determined that the lowest concentration of imidazole able to sufficiently elute the protein from the Ni-NTA column was 200 mM. A two-step elution was performed first with 100 mM imidazole (lane 6) and then with 200 mM imidazole (lane 7). Our Ni-NTA purification of DGKε and DGKε Δ40 contains some contaminating proteins. These contaminants are not detected in Western blots using an anti-His probe (Figure 1), therefore, we visualized the purified fractions with SDS PAGE and silver stain in order to assess purity (Figure 2). The bands corresponding to contaminants in the elution fractions of DGK***ε***-His$_{(6)}$ and DGK***ε***Δ40-His$_{(6)}$ were relatively few and much less intense than the bands corresponding to DGK***ε***-His$_{(6)}$ and DGKεΔ40-His$_{(6)}$. Figure 2 demonstrates that enzymatically cleaving the His$_{(6)}$ epitope tag and eluting the digested protein from a second nickel column effectively removed most of these

contaminants and produced a nearly homogenous sample (Figure 2, Lane 7). The experiments in all of the studies presented here used purified enzyme that did not undergo this additional purification step. The improved purity was not critical for these experiments and required additional time that would have contributed to a greater loss of enzyme activity. Some DGKε Δ40-$His_{(6)}$ can be observed in the flow through and wash fractions (Figure 2, Lanes 2-5).

Purified DGKε and DGKε Δ40 activity and substrate specificity: A mixed micelle assay was conducted to determine if the enzymatic activity of DGKε and DGKε Δ40 purified from Sf21 cells was comparable to the activity levels measured in DGKε transfected Cos7 cells. Proteins in the mixed micelle were allowed to react with ^{32}P radioactively labeled ATP for 10 minutes, and the incorporated ^{32}P was measured in 400 µL of the organic-soluble fraction (Figure 3). A previously reported value for the kinase activity of DGKε transfected Cos7 cells is approximately 0.0045 nmol PA/min/ng of DGKε (*19*). This value is similar to the values we report for Sf21 cell lysates over expressing DGKε (0.0038 ± 0.0003) and DGKε Δ40 (0.0033 ± 0.0003) (Supplementary figure 1). The relative activity of DGKε and DGKε Δ40 in purified form compared to before extraction from Sf21 cell lysates is 0.362 ± 0.108 and 0.279 ± 0.091 respectively (Supplementary figure 1). To determine if DGKε and DGKε Δ40 retain substrate specificity following purification, a mixed micelle assay was conducted to compare18:0/20:4-DAG (SAG) and 18:2/18:2-DAG (DLG) as substrates. The relative activity of DGKε with DLG compared to SAG was 0.441 ± 0.021 and 0.402 ± 0.019 for DGKε Δ40 (Figure 3). The slight difference in specificity between DGKε and DGKε Δ40 was not statistically significant.

Figure 3 also shows that 50% glycerol does not compromise the substrate specificity of DGK***ε*** and DGK***ε*** Δ40 (however, it does stabilize both enzymes dramatically, see below).

DGKε and DGKε Δ40 stability at room temperature: The enzymatic activity of DGK***ε*** and DGK***ε*** Δ40 was measured immediately following purification (0 hours), then at 2 hours, 5.5 hours, 7.5 hours and 9.5 hours after incubation at room temperature to evaluate their stabilities (Figure 4). DGK***ε*** and DGK***ε*** Δ40 began with approximately the same level of enzymatic activity. The activity of DGK***ε*** and DGK***ε*** Δ40 decreased steadily until 7.5 hours and between 7.5 and 9.5 hours, very little additional activity was lost. DGK***ε*** Δ40 retains a significantly higher level of specific enzymatic activity in comparison to DGK***ε***. This trend continues to the last measurement point at 9.5 hours ($p<0.01$). After 2 hours of incubation at room temperature DGK***ε*** and DGK***ε*** Δ40 retained 35% and 50% of their initial activities respectively. By 9.5 hours of incubation, DGK***ε*** retained only 3% of its initial activity and DGK***ε*** Δ40 retained 6%.

DGKε and DGKε Δ40 stability with glycerol at 4^{o}C: The enzymatic activity of DGK***ε*** (Figure 5A) and DGK***ε*** Δ40 (Figure 5B) was measured immediately following purification (0 hours), then at 2 hours, 3 hours, 4.5 hours and 6.5 hours after incubation at 4°C in the presence of 0% and 50% glycerol. Even at 4°C, the activity of both constructs is lost very rapidly (within hours). After 6.5 hours DGKε retained 19% of its initial activity and 48% when stored in 50% glycerol. After 6.5 hours DGKε Δ40 retained 15% of its original activity, in comparison to 38% when stored in 50% glycerol. The stabilizing effect of glycerol on the enzymatic activity of both proteins was determined to be statistically significant ($p<0.01$ in most cases). However, this does not necessarily

mean that glycerol has a greater stabilizing effect on the full length protein, but rather that the full length protein is less stable before the addition of glycerol and hence more of its activity is lost initially.

Effect of freeze thawing on DGKε and DGKε Δ40: The enzymatic activity of DGKε and DGKε Δ40 was measured after successive freeze thaws from -80°C (5 freeze thaws total). Freeze thawing is tremendously damaging to DGKε and DGKε Δ40 activity (Figure 6). The activity of DGKε (Figure 6A) and DGKε Δ40 (Figure 6B) both declined steadily after each successive freeze thaw and by the fourth it did not decrease any further. After a single freeze thaw, DGKε lost 93% of its starting activity and DGKε Δ40 lost 71%. By the fourth freeze thaw, the activity of both DGKε and DGKε Δ40 was reduced to a level comparable to the empty vector control sample, and did not decrease any further after the fifth freeze thaw. For comparison, the activity of a DGKε and DGKε Δ40 aliquot (freeze thawed once) was measured along with the samples that were repeatedly freeze thawed up to five times. The activity of the aliquoted samples (labeled "1 freeze thaw" in Figures 6A and B) remained relatively constant. This control indicates that the difference in activity between samples that were freeze thawed once versus five times is a consequence of freeze thawing, and is not a result of the time the samples spent at -80°C.

Stability of DGKε and DGKε Δ40 at -80°C: The activity of purified DGKε and DGKε Δ40 was tested (using SAG as a substrate) after one day, two days, one week, two weeks, four weeks, and fourteen weeks of storage at -80°C (Figure 7A and B). All of the samples were freeze thawed only once. Both the activity of DGKε (Figure 7A) and DGKε Δ40

(Figure 7B) did not change significantly over a fourteen-week period of storage at -80°C, thus the major cause for the drop in activity can be attributed to the single freeze thaw.

Effect of glycerol on DGKε and DGKε Δ40 at -80°C: The activity of purified DGKε and DGKε Δ40 after one day, two days, one week, two weeks, four weeks, and fourteen weeks of being stored at -80°C was compared to the enzymes stored in 25% glycerol and 50% glycerol (Figure 7 and B). Both DGKε and DGKε Δ40 retained a significantly higher amount of their initial activity over time when stored in glycerol (Figure 7A and 7B). The activity of protein stored without glycerol declined to less than 5% of its original activity after just two days of storage at -80°C. In contrast, the samples with glycerol retained at least half of their original activity levels. A subtle downward trend is observed with the samples stored in 25% glycerol, but the activity of samples stored with 50% glycerol held constant for at least fourteen weeks. Therefore, the activity loss between zero hours and fourteen weeks appears to largely be a result of the single freeze thaw, and not a consequence of being stored at -80°C for 14 weeks. To ensure that storing DGKε and DGKε Δ40 in 50% glycerol does not compromise substrate specificity, we measured their activity with SAG and DLG substrates (Figure 3). 50% glycerol did not alter the substrate specificity of DGKε or DGKε Δ40. We also measured the activity of freshly purified DGKε and DGKε Δ40 immediately after adding 50% glycerol to show that it did not cause any artifacts in the mixed-micelle activity assay and there were no differences between these freshly purified proteins in 0% versus 50% glycerol when both SAG and DLG are used as substrates (Figure 8).

DGKε and DGKε Δ40 secondary structure characterization: Circular dichroism spectroscopy was performed from 260nm-196nm on DGK***ε*** and DGK***ε*** Δ40 to compare the components of their secondary structures. DGK***ε*** and DGK***ε*** Δ40 have very similar CD wavelength spectra (Figure 9). The mean residue ellipticity for DGK***ε*** and DGK***ε*** Δ40 is shown as the average of three independent purifications in Figure 9. DGK***ε*** Δ40 exhibited much greater stability with a mean residue ellipticity consistently reaching -10,000 degrees x cm^2/dmol. In contrast, DGK***ε*** was much less stable and exhibited more variability between preparations, sometimes reaching close to -15,000 degrees x cm^2/dmol. Analysis with CDPro software using the average of three independent purifications reveals that the secondary structure of DGK***ε*** is comprised of 29% α-helices and 22% β-strands, and DGK***ε*** Δ40 is 30% α-helices and 21% β-strands.

DGKε and DGKε Δ40 thermal denaturation curves: Circular dichroism spectroscopy was used to monitor the thermal denaturation DGK***ε*** and DGK***ε*** Δ40 between 20°C and 100°C and upon cooling back to 20°C at 222 nm. The effect of different concentrations of glycerol, as well as the presence or absence of DOPC on thermostability was recorded. In 20% glycerol, both proteins exhibited a biphasic transition from the folded to unfolded states (Figure 10 A & C). The transitions occurred at 56°C and 77°C for both proteins. The addition of DOPC in a 50:1 molar ratio (lipid: protein) along with 20% glycerol did not change the first transition for either protein (it remained at 56°C). DOPC resolved the two transition points of DGKε Δ40 and shifted the higher one from 77°C to 92°C (Figure 10 D). DOPC did not change the lower transition point of DGKε either, however, it made the second transition slightly broader (Figure 10 B). In contrast, increasing the glycerol

percentage from 20% to 50% increased the cooperativeness of the unfolding process and resolved the two transition temperatures. With 50% glycerol, the transition temperatures became sharper and shifted to approximately 30°C and 80°C for both proteins (Figure 11 A & C). 50% glycerol also caused the thermal unfolding to be ~80% reversible, in contrast to the irreversibility of the transition in the absence of 50% glycerol (Figure 11 A & C). DOPC with 50% glycerol increased the first transition of DGKε from 29°C to 35°C and effectively made the second transition very broad (Figure 11 B). DOPC and 50% glycerol broadened both the high and low temperature transition point of DGKε Δ40 (Figure 11 D). The degree of refolding was essentially the same for DGKε and DGKε Δ40 in 50% glycerol versus 50% glycerol with DOPC.

DISCUSSION

We have successfully expressed human DGKε and DGKε Δ40 containing a C-terminal $His_{(6)}$ tag using baculovirus infected Sf21 insect cells carrying the corresponding genes. The $His_{(6)}$ tag was used for purifying the proteins with nickel affinity chromatography. The isolated protein retained a high level of enzymatic activity as well as specificity for SAG as a substrate. However, it was found that the purified enzyme quickly loses activity upon storage and as a result of freezing and thawing cycles. We therefore proceeded to truncate the enzyme at the amino terminus to remove the most hydrophobic segment of the protein, residues 20-40. The purpose of this was to increase the overall solubility of DGKε and reduce the tendency of purified DGKε to self-associate into inactive aggregates. It was previously found that N-terminally truncated forms of DGKε, expressed in Cos-7

cells and containing an N-terminal Flag epitope tag, were both active and showed substrate specificity for SAG (*3;12*), missing 40 or 58 residues, respectively. We therefore expressed a truncated DGKε omitting 40 N-terminal residues and containing a C-terminal hexa-His tag. Expression and purification of this construct was carried out with the same procedure followed for the corresponding full length DGKε. Both the full length and truncated forms of DGKε exhibited the same level of substrate specificity (Figure 3). This finding is similar to our previous findings using N-terminal Flag tag constructs, expressed in Cos-7 cells (*3;12*). The similarity of the properties of the different constructs suggests that neither the activity nor the specificity of the enzyme is critically affected by the nature or position of the epitope tag, or by the presence of other cellular components in the impure preparations from Cos-7 cells (at least in the context of a detergent-phospholipid mixed micelle assay).

Both the full length and N-terminally truncated forms lost significant activity on storage at room temperature, 4°C, -80°C as well as with freeze/thaw cycles. This is in contrast with the crude cell pellets of Cos-7 cells that over-expressed these proteins and retained full activity at -80°C for several months. However, comparing the purified full length DGKε-$His_{(6)}$ with the DGK$\varepsilon\Delta$40-$His_{(6)}$, the truncated form missing the N-terminal hydrophobic segment exhibited slightly enhanced stability compared to the full-length form (Figure 4). We performed DLS to measure the oligomerization status of DGKε to try to determine to what extent aggregation was causing the dramatic losses in kinase activity. The results reveal that DGKε exists

98% as a monomer and only 2% as larger aggregates. This strongly suggests that there is minimal aggregation of DGKε, and this process is likely a minor factor contributing to its instability.

Our visualization of the purified fractions with SDS PAGE and silver stain shows a very homogenous preparation of DGK$\varepsilon\Delta$40 (Figure 2). Ni-NTA columns with bound DGK$\varepsilon\Delta$40-$His_{(6)}$ were washed three times with buffer containing 40 mM imidazole to remove contaminating proteins, which also resulted in some DGK$\varepsilon\Delta$40-$His_{(6)}$ being washed off of the column (Figure 2, lanes 1 and 2). The amount of imidazole in the wash steps can be adjusted to increase yield, but would compromise purity. The amount of imidazole in the equilibration buffer can also be reduced (we used 20 mM) to prevent loss of DGK$\varepsilon\Delta$40-$His_{(6)}$ in the flow through. The DGK$\varepsilon\Delta$40-$His_{(6)}$ present in the flow through and wash fractions can also be purified in another column to increase yield.

Until now, no studies have investigated the structure or conformational properties of DGKε and very little was known beyond its primary structure. We have used CD to obtain the first estimates of the secondary structure content and architecture of DGKε and DGKε Δ40. The conformational properties of the two DGKε proteins are very similar, at least by the criterion of CD (Figure 9). Secondary structure estimations with these spectra using CDPro software also give similar values for the two proteins (Table 1) and shows that the protein has significant α-helical and β-structure content. Secondary structure predictions using the program I-TASSER (*20;21;22*) generated values of 25% α-helix and 21% β-structure, in excellent agreement with the values estimated by CD (29%α-helix

and 22% β-structure). There is also a DGK from *Staphylococcus aureus*, dgkB, that shows some homology to several mammalian DGK isoforms, and whose crystal structure is known (*23*). Secondary structure annotations on the UniProtKB/Swiss-Prot site for dgkB (Accession number Q6GFF9) give values of 21.9% and 34% for α-helical and β-structure, respectively. Secondary structure analysis by CD is known to be most reliable for α-helices. Estimates of helical content are in reasonable agreement for DGK$\boldsymbol{\varepsilon}$ using analysis of the CD spectra (29%), the I-TASSER predictive program (25%) as well as for the dgkB based on the crystal structure (22%). The β-structure analysis by CD (22%) is nearly identical to the prediction from the I-TASSER server (21%) and both are lower than the β-structure reported for dgkB (34%). This is not surprising based on the differences in the primary amino acid sequence of DGK$\boldsymbol{\varepsilon}$ and dgkB.

Thermal denaturation of the proteins was monitored using the temperature dependence of the mean residue ellipticity at 222 nm in the presence or absence of a 50:1 molar ratio (lipid to protein) of DOPC and varying concentrations of glycerol. We show that DGK$\boldsymbol{\varepsilon}$ and DGK$\boldsymbol{\varepsilon}$ Δ40 have almost identical thermal denaturation patterns in 20% glycerol, and that they unfold in a biphasic manner with the first transition occurring at 56°C and the second at 77°C (Figure 10 A & C). Upon adding DOPC (a non-substrate lipid) the first transition remained unchanged at 56°C. In contrast, the second transition of DGK$\boldsymbol{\varepsilon}$ Δ40 shifted to 92°C and for DGK$\boldsymbol{\varepsilon}$ it became very broad. This seems to suggest that the first transition corresponds to a region of the protein that is not involved in lipid binding, at least not the lipid DOPC. In contrast, the region of the protein corresponding to the second transition does seem to bind DOPC. It is not surprising that DOPC interacts

differently with the two proteins considering that the 40 residues corresponding to a membrane-associating alpha helix is absent in the DGKε Δ40 protein. The broadening of the second transition seen in DGKε suggests that the corresponding region of the protein binds DOPC in a stabilizing manner and likely does not completely unfold; even at 100°C (this level of stability during thermal denaturation is not uncommon for hydrophobic alpha helices). In contrast, the same region in DGKε Δ40 interacts with DOPC such that it unfolds in a very cooperative process at 92°C (Figure 10 D). These results are in agreement with the output from the PSIPRED server, which suggests that DGKε is comprised of two domains (*24*). The biphasic denaturation of DGKε observed with CD is consistent with the idea of DGKε comprising two domains with different thermal stabilities. The higher temperature transition most likely corresponds to the domain comprised of membrane-associating alpha helices while the other domain corresponding to the less stable transition likely possesses a higher degree of disordered structure. CD revealed that the domain of DGKε corresponding to the higher temperature transition is the one that interacts with DOPC, therefore, this region of the protein is likely the domain with hydrophobic alpha helices, as these structures are known to demonstrate exceptional thermal stability. In contrast, the lower temperature transition was unaffected by the addition of DOPC, which would be expected of a less stable disordered domain that does not interact specifically with lipid.

The results of increasing the glycerol percentage to 50% are unexpected. There are still two transition temperatures, but they are much more resolved and sharper, and they appear at different temperatures compared to 20% glycerol. For both proteins, the

first transition temperature shifted to approximately 30°C and the second to just over 80°C. It is not entirely clear why the additional glycerol shifted the lower temperature transition to a lower temperature, while the higher transition temperature shifted up. 77°C is not dramatically different from 81°C and 83°C so it seems that the region of the proteins corresponding to this transition was marginally stabilized by the additional glycerol and consequently denatured at a slightly higher temperature. However, this logic does not explain the shift of the lower transition temperature from 56°C to 29°C for DGKε and 31°C for DGKε Δ40. It is possible that the additional glycerol stabilized a conformation with a much lower transition temperature and it unfolded in a very cooperative process to give rise to the lower transition observed. The overall shapes of the denaturation curves with 50% do in fact reflect a more cooperative process. 50% glycerol also facilitated partial refolding of both proteins, which is a well-established characteristic of the polyol. The thermal denaturation of these proteins with 50% glycerol and DOPC shows that the lipid was still able to interact with both enzymes despite the high concentration of glycerol. This is evident from the broadening of the transition temperatures. This suggests that DOPC does in fact bind with relatively high affinity to DGKε and DGKεΔ40 and alters their stability during thermal denaturation. DGKε and DGKε Δ40 have almost identical thermal denaturation patterns in 20% glycerol and their patterns remain nearly identical in 50% glycerol (yet the 20% and 50% spectra are very distinct from one another). This suggests that glycerol interacts with both proteins but not in a specific manner. In contrast, adding DOPC to these proteins gives rise to differences in their spectra suggesting that the lipid forms specific interactions, which differ between

the two proteins. The slight loss of ellipticity with 50% glycerol is ~80% reversible upon cooling and is similar for both proteins. Therefore, glycerol is an important stabilizing agent and was included into the purification protocol and added to samples prior to storage. However, the loss of ellipticity in 20% glycerol (both with and without DOPC, Figure 10) is irreversible and the structure is not regained after cooling. The gradual and irreversible nature of the loss of structure upon heating suggests that it is most likely caused by protein aggregation, rather than, or in addition to an unfolding of a monomeric protein. In fact, protein aggregates were visible in the cuvette following all of the thermal denaturation experiments except for the cases where 50% glycerol was used.

Before the purification protocol was optimized, DGKε and DGKε Δ40 were eluted with more than 200 mM imidazole, the elution times were longer than the necessary one to two hours, and glycerol and β-mercaptoethanol were absent from the buffers. Thermal denaturation curves with these preparations comparing 0% glycerol and no DOPC to the presence of DOPC showed interesting differences. Of particular interest is the observation of a sharper, more cooperative thermal transition of the truncated protein in the presence of DOPC at about 90°C (data not shown). This transition was partially reversible on cooling. This refolding occurred over a slightly lower temperature range, likely because of kinetic effects. This sharp, cooperative transition observed at 90°C was only observed with the truncated protein and not the full length form and is most apparent with DOPC present. The marked effect of lipid on the thermal properties of DGK$\varepsilon\Delta$40 is evidence that even the truncated protein binds to lipid, possibly preventing some aggregation and thus allowing the denaturation process to be observed. A possible

reason that it was not observed to the same extent with the full length protein in the presence of DOPC may be because the longer protein undergoes this transition above 100°C or that the full length protein has a greater tendency to aggregate and therefore falls out of solution before the denaturation process can be measured.

The present work presents a method for extracting milligram amounts of pure and active DGKε from only 4 T175 flasks of Sf21 cells. This enzyme has properties that are unique among the 10 mammalian isoforms of DGK. The unique property of specificity for SAG suggests that this enzyme plays an important role in the phosphatidylinositol cycle. The present work shows that this property is intrinsic to the enzyme and is not dependent on the presence of other factors present in the crude membrane preparations used previously to study this protein. However, the purified preparation exhibits less stability on storage than the unpurified preparation from mammalian cells. This can be partially ameliorated by cloning an N-terminally truncated form of DGKε and using glycerol in the enzyme preparations.

We have initially characterized the protein using CD. Secondary structure analysis of the CD spectra shows that the protein contains significant amounts of both α-helical and β-structure. The secondary structure content resembles that of the prokaryotic dgkB as well as secondary structure predictions based on the sequence. Both constructs exhibit a biphasic thermal denaturation and bind to the lipid DOPC. 50% glycerol facilitates the partial refolding of both enzymes and increases the cooperativeness of the transitions from the folded to unfolded states. The lack of a cooperative denaturation transition of this protein at lower temperatures in conditions lacking glycerol and DOPC is

characteristic of membrane proteins and is consistent for the strong affinity this protein has for membranes (*12*). The purification of DGKε will assist in many new discoveries surrounding the structure and function of this critical enzyme with important implications for DGKε-related diseases.

References

1. Shulga, Y. V., Topham, M. K., and Epand, R. M. (2011) Regulation and functions of diacylglycerol kinases, *Chem. Rev.111*, 6186-6208.
2. Tang, W., Bunting, M., Zimmerman, G. A., McIntyre, T. M., and Prescott, S. M. (1996) Molecular cloning of a novel human diacylglycerol kinase highly selective for arachidonate-containing substrates, *J. Biol. Chem.271*, 10237-10241.
3. Lung, M., Shulga, Y. V., Ivanova, P. T., Myers, D. S., Milne, S. B., Brown, H. A., Topham, M. K., and Epand, R. M. (2009) Diacylglycerol kinase epsilon is selective for both acyl chains of phosphatidic acid or diacylglycerol, *J. Biol. Chem.284*, 31062-31073.
4. Rodriguez de Turco, E. B., Tang, W., Topham, M. K., Sakane, F., Marcheselli, V. L., Chen, C., Taketomi, A., Prescott, S. M., and Bazan, N. G. (2001) Diacylglycerol kinase epsilon regulates seizure susceptibility and long-term potentiation through arachidonoyl- inositol lipid signaling, *Proc. Natl. Acad. Sci. U. S. A98*, 4740-4745.
5. Milne, S. B., Ivanova, P. T., Armstrong, M. D., Myers, D. S., Lubarda, J., Shulga, Y. V., Topham, M. K., Brown, H. A., and Epand, R. M. (2008) Dramatic differences in the roles in lipid metabolism of two isoforms of diacylglycerol kinase, *Biochemistry47*, 9372-9379.
6. Zhang, N., Li, B., Al-Ramahi, I., Cong, X., Held, J. M., Kim, E., Botas, J., Gibson, B. W., and Ellerby, L. M. (2012) Inhibition of lipid signaling enzyme diacylglycerol kinase epsilon attenuates mutant huntingtin toxicity, *J. Biol. Chem.287*, 21204-21213.

7. Ozaltin, F., Li, B., Rauhauser, A., An, S. W., Soylemezoglu, O., Gonul, I. I., Taskiran, E. Z., Ibsirlioglu, T., Korkmaz, E., Bilginer, Y., Duzova, A., Ozen, S., Topaloglu, R., Besbas, N., Ashraf, S., Du, Y., Liang, C., Chen, P., Lu, D., Vadnagara, K., Arbuckle, S., Lewis, D., Wakeland, B., Quigg, R. J., Ransom, R. F., Wakeland, E. K., Topham, M. K., Bazan, N. G., Mohan, C., Hildebrandt, F., Bakkaloglu, A., Huang, C. L., and Attanasio, M. (2013) DGKE Variants Cause a Glomerular Microangiopathy That Mimics Membranoproliferative GN, *Journal of the American Society of Nephrology24*, 377-384.

8. Lemaire, M., Fr+¬meaux-Bacchi, V., Schaefer, F., Choi, M., Tang, W. H., Quintrec, M. L., Fakhouri, F., Taque, S., Nobili, F., Martinez, F., Ji, W., Overton, J. D., Mane, S. M., N++rnberg, G., Altm++ller, J., Thiele, H., Morin, D., Deschenes, G., Baudouin, V., Llanas, B., Collard, L., Majid, M. A., Simkova, E., N++rnberg, P., Rioux-Leclerc, N., Moeckel, G. W., Gubler, M. C., Hwa, J., Loirat, C., and Lifton, R. P. (2013) Recessive mutations in DGKE cause atypical hemolytic-uremic syndrome, *Nature Genetics45*, 531-536.

9. Niizeki, T., Takeishi, Y., Kitahara, T., Arimoto, T., Ishino, M., Bilim, O., Suzuki, S., Sasaki, T., Nakajima, O., Walsh, R. A., Goto, K., and Kubota, I. (2008) Diacylglycerol kinase-epsilon restores cardiac dysfunction under chronic pressure overload: a new specific regulator of Galpha(q) signaling cascade, *Am. J. Physiol Heart Circ. Physiol295*, H245-H255.

10. Liu, K., Kunii, N., Sakuma, M., Yamaki, A., Mizuno, S., Sato, M., ... & Okabe, T. (2016).Identification and characterization of a novel diacylglycerol kinase α-selective inhibitor, CU-3.*Journal of Lipid Research*, jlr-M062794

11. Walsh, J. P., Suen, R., Lemaitre, R. N., and Glomset, J. A. (1994) Arachidonoyl-diacylglycerol kinase from bovine testis. Purification and properties, *J. Biol. Chem.269*, 21155-21164.

12. Dicu, A. O., Topham, M. K., Ottaway, L., and Epand, R. M. (2007) Role of the hydrophobic segment of diacylglycerol kinase epsilon, *Biochemistry46*, 6109-6117.

13. Krogh, A., Larsson, B., Von Heijne, G., &Sonnhammer, E. L. (2001). Predicting transmembrane protein topology with a hidden Markov model: application to complete genomes. *Journal of molecular biology*, *305*(3), 567-580.

14. Sonnhammer, E. L., Von Heijne, G., & Krogh, A. (1998, July). A hidden Markov model for predicting transmembrane helices in protein sequences. In *Ismb* (Vol. 6, pp. 175-182).

15. Nørholm, M. H., Shulga, Y. V., Aoki, S., Epand, R. M., & von Heijne, G. (2011). Flankingresidues help determine whether a hydrophobic segment adopts a monotopic or bitopic topology in the endoplasmic reticulum membrane. *Journal of Biological Chemistry*, *286*(28), 25284-25290.

16. Decaffmeyer, M., Shulga, Y.V., Dicu, A.O., Thomas, A., Truant, R., Topham, M.K., Brasseur, R. and Epand, R.M., 2008. Determination of the topology of the hydrophobic segment of mammalian diacylglycerol kinasesepsilon in a cell

membrane and its relationship to predictions from modeling.*Journal of molecular biology*, *383*(4), pp.797-809.

17. Matsui, H., Hozumi, Y., Tanaka, T., Okada, M., Nakano, T., Suzuki, Y., ... &Goto, K. (2014). Role of the N-terminal hydrophobic residues of DGKε in targeting the endoplasmic reticulum.*Biochimicaet BiophysicaActa (BBA)-Molecular and Cell Biology of Lipids*, *1841*(10), 1440-1450.
18. Prodeus, A., Berno, B., Topham, M. K., and Epand, R. M. (2013) The basis of the substrate specificity of the epsilon isoform of human diacylglycerol kinase is not a consequence of competing hydrolysis of ATP, *Chem. Phys. Lipids166*, 26-30.
19. D'Souza, K., & Epand, R. M. (2012). Catalytic Activity and Acyl-Chain Selectivity of Diacylglycerol Kinase ε Are Modulated by Residues in and near the Lipoxygenase-Like Motif. *Journal of molecular biology*, *416*(5), 619-628.
20. Roy, A., Kucukural, A., and Zhang, Y., 2010. I-TASSER: a unified platform for automatedprotein structure and function prediction. Nat Protoc. 5, 725-738.
21. Yang, J., Yan, R., Roy, A., Xu, D., Poisson, J., and Zhang, Y., 2015. The I-TASSER Suite:protein structure and function prediction. Nature Methods 12, 7-8.
22. Zhang, Y., 2008. I-TASSER server for protein 3D structure prediction. BMC Bioinformatics. 9,40.
23. Miller, D. J., Jerga, A., Rock, C. O., and White, S. W. (2008) Analysis of the Staphylococcus aureus DgkB structure reveals a common catalytic mechanism for the soluble diacylglycerol kinases, *Structure.16*, 1036-1046.
24. Jennings, W., Doshi, S., D'Souza, K., & Epand, R. M. (2015). Molecular properties

of diacylglycerol kinase-epsilon in relation to function. *Chemistry and physics of lipids*, *192*, 100-108.

Figures:

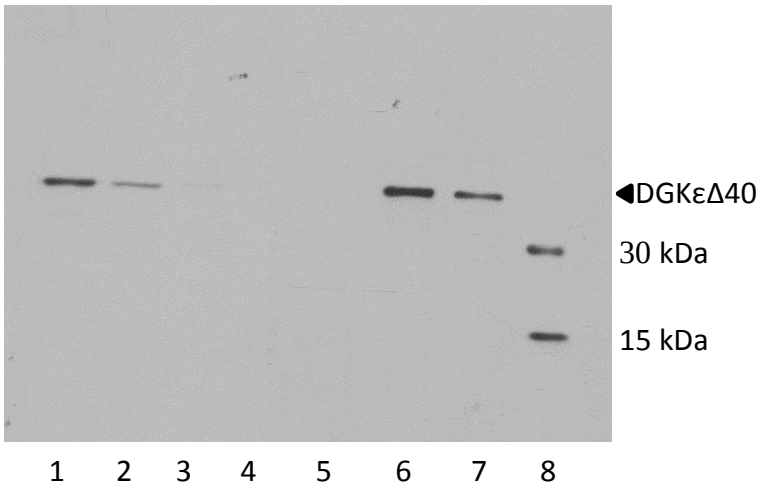

Figure 1: *Detection of DGKε Δ40-His$_{(6)}$ with Anti-His$_{(6)}$ antibody following Ni-NTA column chromatography purification.* An intense 64 kDa DGKεΔ40-His$_{(6)}$ band was detected in lane 1 (lysate), and a considerably less intense band was detected in lane 2 (flow through). Lanes 3, 4 and 5 do not contain any intense bands, and correspond to the three wash fractions. Lane 6 with an intense DGKεΔ40-His$_{(6)}$ band corresponds to the first elution fraction (100mM imidazole), while lane 7 with a slightly less intense band shows the second elution fraction (200mM imidazole). Lane 8 is a molecular weight marker.

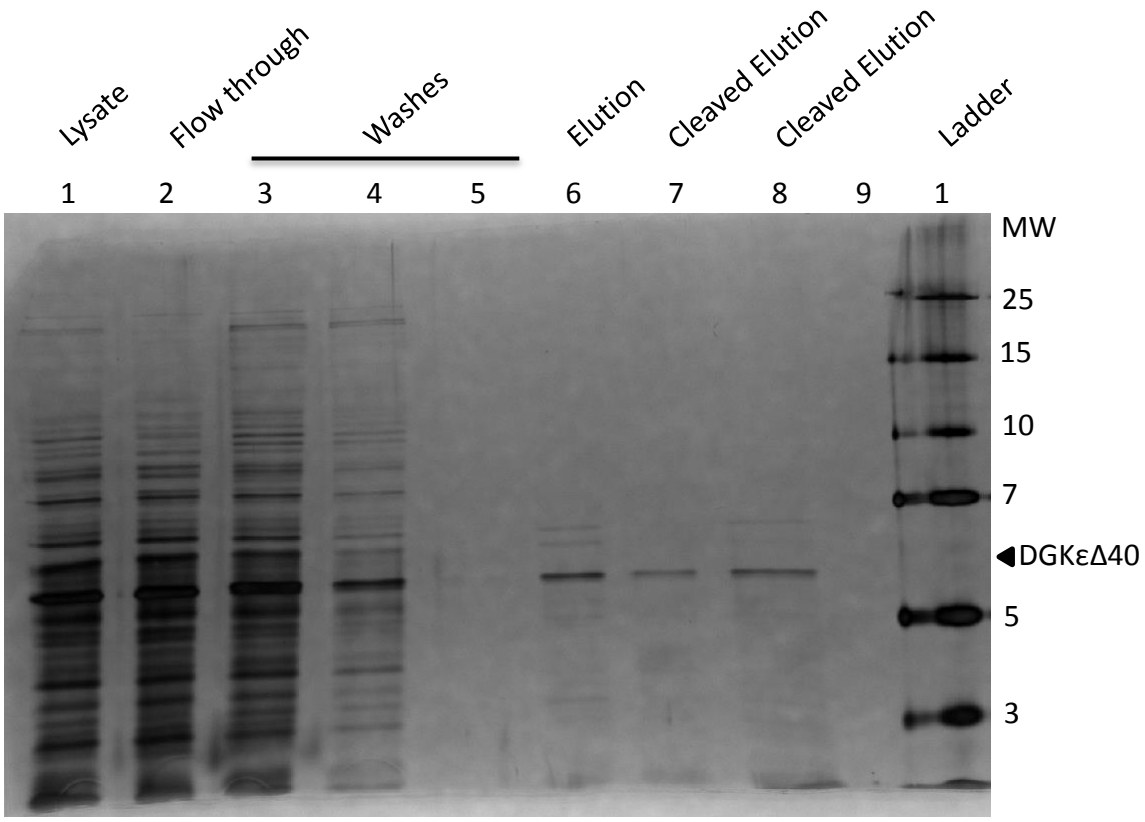

Figure 2: *Visualization of Ni NTA purified DGKε Δ40-His$_{(6)}$ with SDS PAGE (7.5% Acrylamide) and silver stain.* DGKεΔ40-His$_{(6)}$ was purified in a 10mL column pre-equilibrated with 30mM imidazole, wash fractions contained 40mM imidazole, and elution fractions contained ~150mM imidazole. The His$_{(6)}$ was cleaved with AcTEV protease (ThermoFisher Scientific) following elution and the digested sample was loaded into a second Ni-NTA column and the flow-through was subsequently collected. Lane 1- Sf21 cell lysate, Lane 2- Column flow-through, Lane 3- Wash 1, Lane 4- Wash 2, Lane 5- Wash 3, Lane 6- Eluted DGKεΔ40-His$_{(6)}$, Lane 7- digested DGKεΔ40 flow-through, Lane 8- digested DGKεΔ40 flow-through (concentrated).

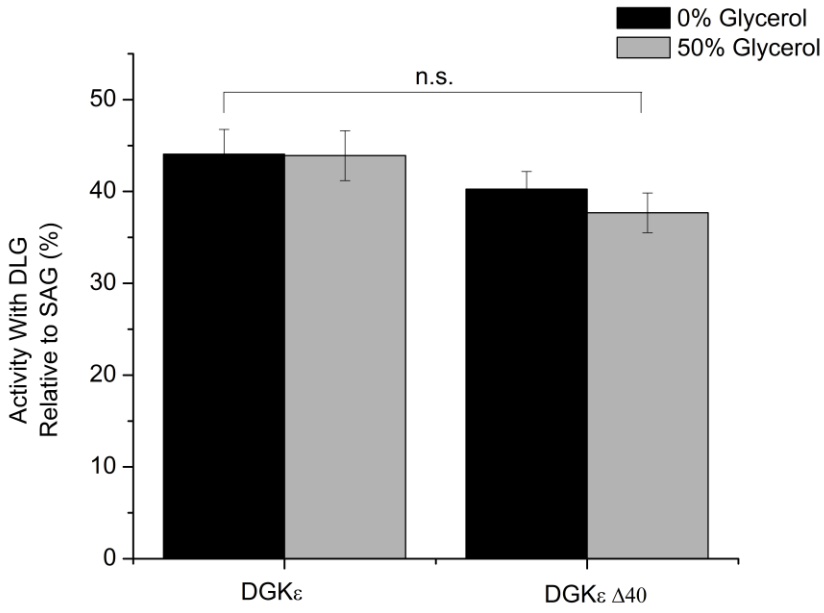

Figure 3: *Purified DGKε-His$_{(6)}$ and DGKε Δ40-His$_{(6)}$ demonstrate substrate specificity between SAG and DLG substrates in both 0% and 50% glycerol.* Protein samples purified by Ni-NTA chromatography containing 0% glycerol were compared to samples containing 50% glycerol. Protein samples were incorporated into a mixed micelle consisting of Triton X-100, DOPC and either SAG or DLG. The enzymatic activity of DGKε-His$_{(6)}$ and DGKε Δ40-His$_{(6)}$ was significantly higher with SAG as a substrate and this was not affected by the addition of 50% glycerol. DGKε Δ40-His$_{(6)}$ appears to display slightly higher preference for the SAG substrate, however, it is not statistically significant at a 95% confidence interval ($P>0.05$). Data is presented as means ± SEM, ($N=4$, $n=12$).

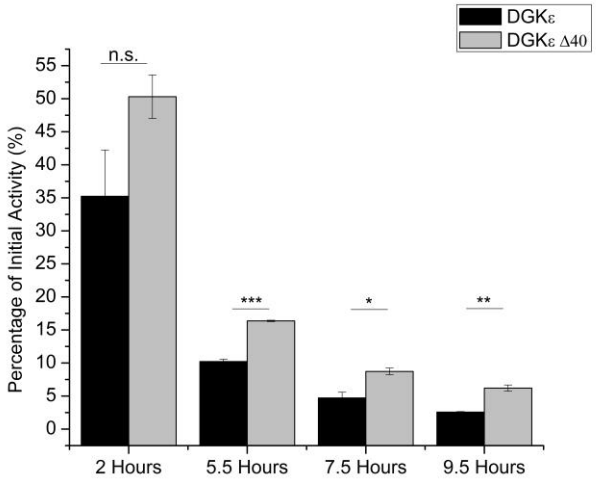

Figure 4: *Comparison of purified DGKε-His$_{(6)}$ and DGKε Δ40-His$_{(6)}$ activity over 9.5 hours of incubation at Room Temperature.* Enzymatic activities was calculated (nmol PA/min/ng of purified DGKε-His$_{(6)}$ or DGKε Δ40-His$_{(6)}$) and were adjusted using empty vector transfected Sf21 cells. The activity is presented as a percentage of the activity level of freshly purified enzyme at time zero. The difference between DGKε-His$_{(6)}$ and DGKε Δ40-His$_{(6)}$ are statistically significant (*=P < 0.05, **=P < 0.01, ***=P < 0.0001). Data is presented as means ± SEM and is representative of three independent experiments.

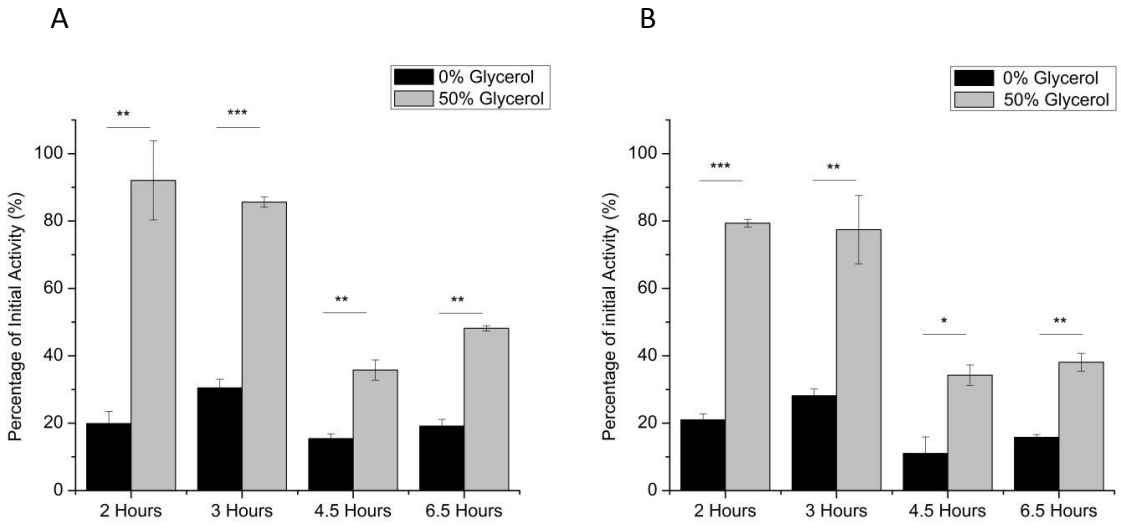

Figure 5: *Comparison of specific enzymatic activity of (A) DGKε-His$_{(6)}$ and (B) DGKε Δ40-His$_{(6)}$ in the presence of 0% and 50% glycerol at 4°C.* Enzymatic activities were calculated (nmol PA/min/ng of purified DGKε-His$_{(6)}$ or DGKε Δ40-His$_{(6)}$) and were adjusted using empty vector transfected Sf21 cells. The activity is presented as a percentage of the activity level of freshly purified enzyme at time zero. The differences between 0% glycerol and 50% glycerol are statistically significant for both DGKε-His$_{(6)}$ and DGKε Δ40-His$_{(6)}$ (*=P < 0.05, **=P < 0.01, ***=P < 0.0001). Data is presented as means ± SEM and is representative of three independent experiments.

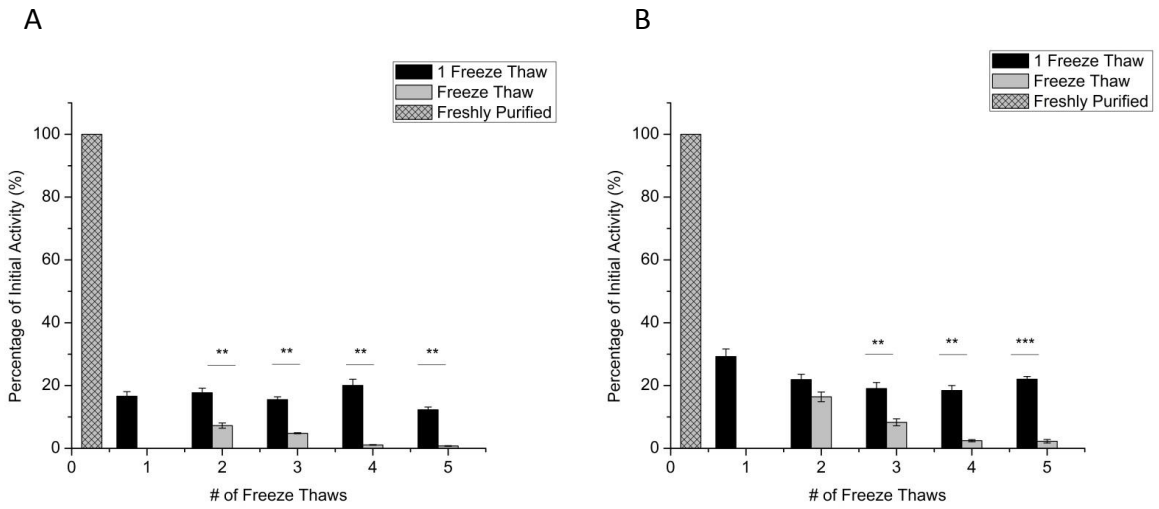

Figure 6: *Effect of freeze thawing on the enzymatic activity of (A) DGKε-His$_{(6)}$ and (B) DGKε Δ40-His$_{(6)}$.* Specific activities were calculated (nmol PA/min/ng of purified DGKε-His$_{(6)}$ or DGKε Δ40-His$_{(6)}$) and were adjusted using empty vector transfected Sf21 cells. The activity is presented as a percentage of the activity level of freshly purified enzyme at time zero. A control sample was freeze thawed once "1 freeze thaw" and the "freeze thaw" samples were freeze thawed 2, 3, 4 or 5 times. Freeze thawing proved extremely damaging to specific enzymatic activity (*=P < 0.05, **=P < 0.01, ***=P < 0.0001). Data is presented as means ± SEM and is representative of three independent experiments.

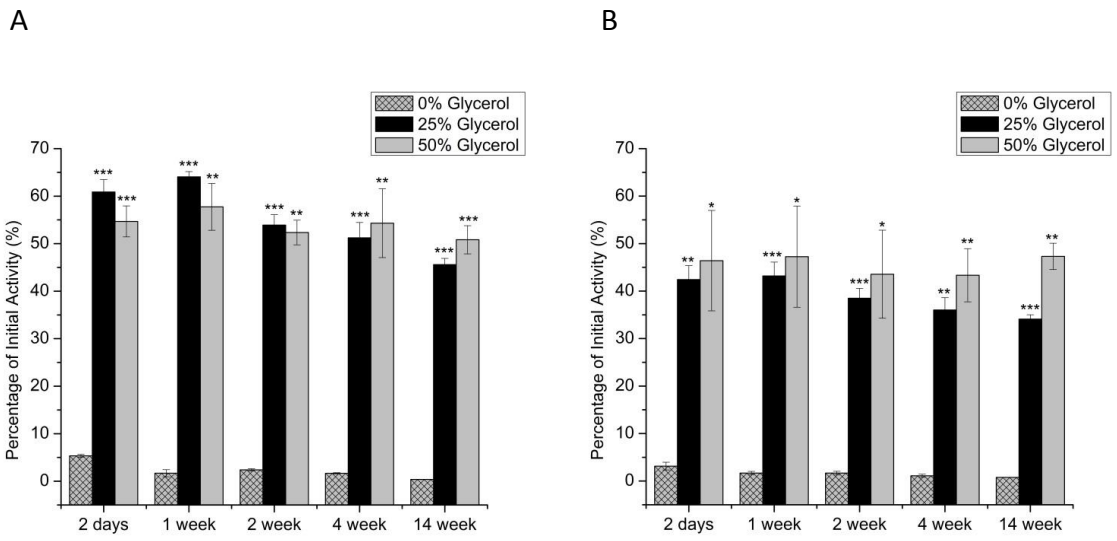

Figure 7: *Comparison of the effects of storage at -80°C on (A) DGKε-His$_{(6)}$ and (B) DGKε Δ40-His$_{(6)}$ in the presence of 0%, 25% and 50% glycerol.* Enzymatic activities were calculated (nmol PA/min/ng of purified DGKε-His$_{(6)}$ or DGKε Δ40-His$_{(6)}$) and were adjusted using empty vector transfected Sf21 cells. The activity is presented as a percentage of the activity level of freshly purified enzyme at time zero. Glycerol drastically minimizes the damage done by freeze thawing (*=P < 0.05, **=P < 0.01, ***=P < 0.0001). Data is presented as means ± SEM and is representative of three independent experiments.

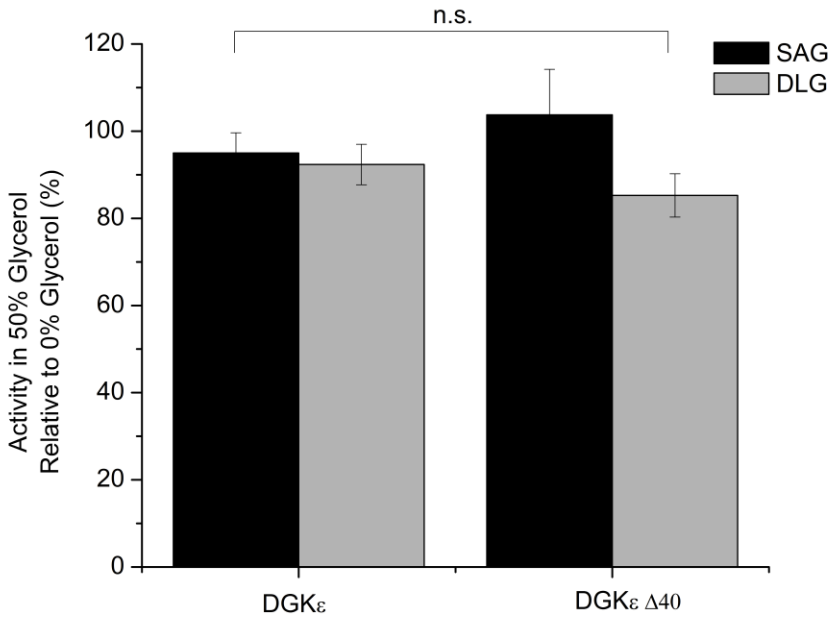

Figure 8: *Freshly purified DGKε-His$_{(6)}$ and DGKε Δ40-His$_{(6)}$ demonstrate the same lack of effect of 50% glycerol with SAG and DLG as substrates.* Protein samples were purified by Ni-NTA chromatography, stored in 50% glycerol and incorporated into a mixed micelle consisting of Triton X-100, DOPC and either SAG or DLG. Enzymatic activities were calculated (nmol PA/min/ng of purified DGKε-His$_{(6)}$ or DGKε Δ40-His$_{(6)}$) and were adjusted using empty vector transfected Sf21 cells. The activity is presented as a percentage of the activity level of freshly purified enzyme at time zero in 0% glycerol. Data is presented as means ± SEM, N=6, n=18 for SAG and N=3, n=9 for DLG.

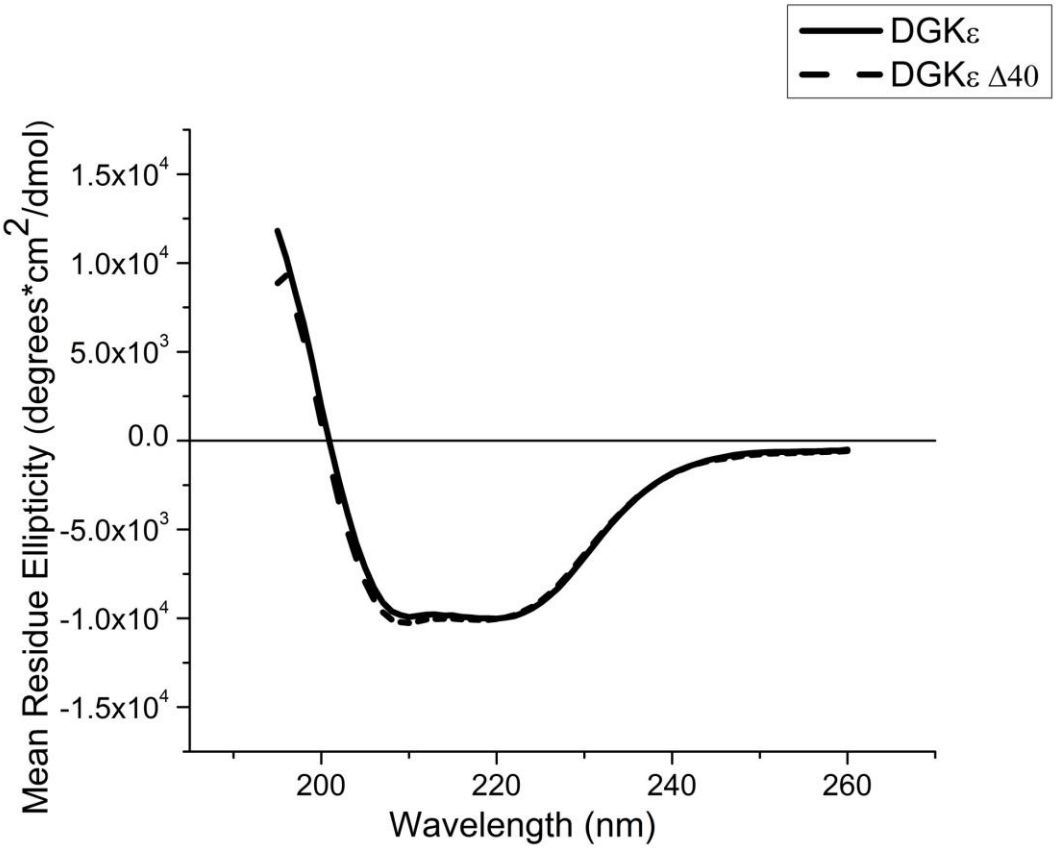

Figure 9: *Figure 11: Comparison of DGKε-His$_{(6)}$ and DGKε Δ40-His$_{(6)}$ with Circular Dichroism spectroscopy.* CD spectra were measured from 260nm to195nm in 1nm increments and a 5 second averaging time. The DGKε-His$_{(6)}$ and DGKεΔ40-His$_{(6)}$ spectra represent averages of three independent purifications. Data is presented in units of mean residue ellipticity and was plotted with OrginPro 8 Software, smoothened with the Adjacent-Averaging method.

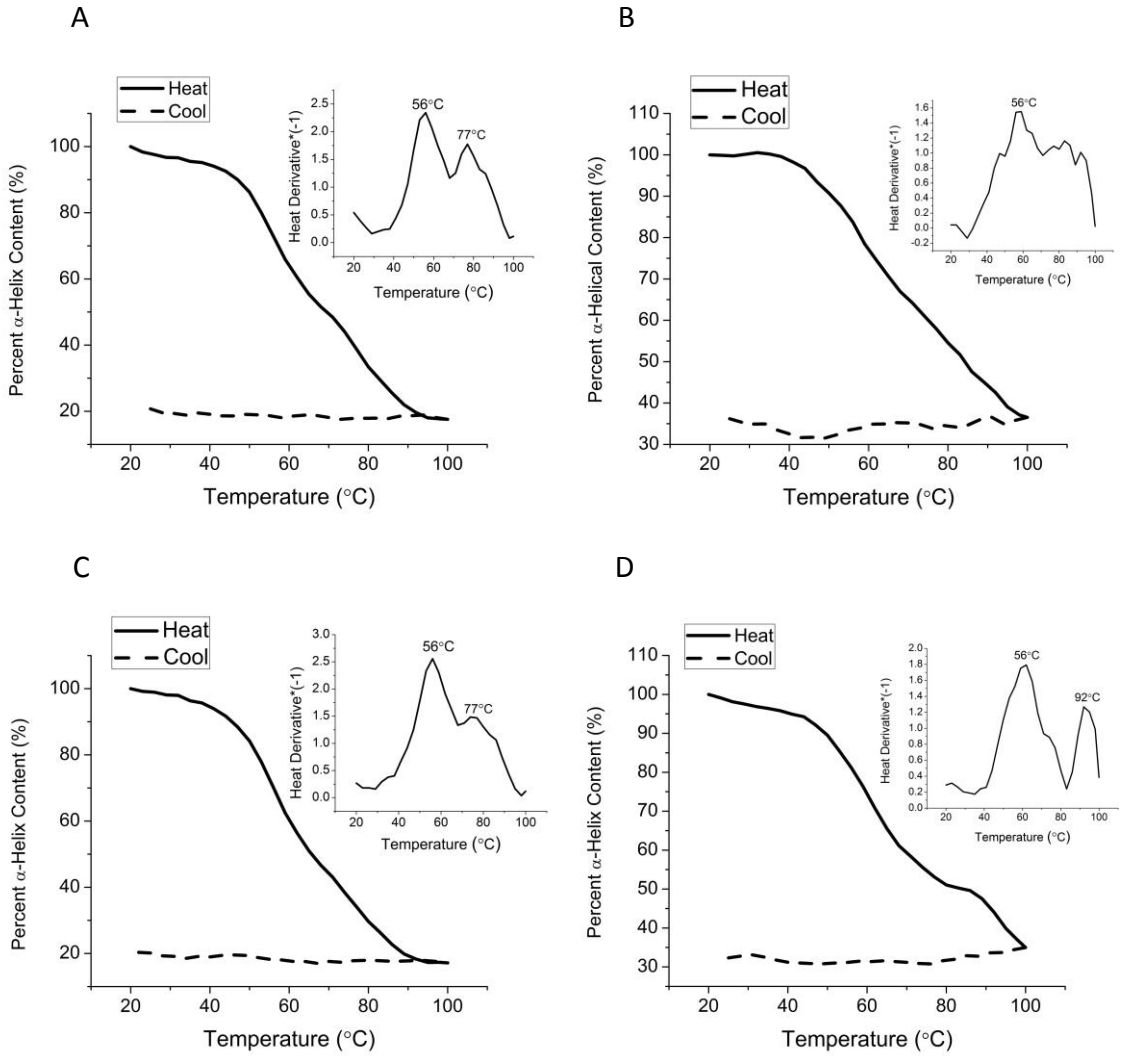

Figure 10: *Thermal denaturation of DGKε-His$_{(6)}$ with (A) 20% glycerol (B) 20% glycerol with 50:1 molar ratio DOPC (lipid:protein) and DGKε Δ40-His$_{(6)}$ with (C) 20% glycerol and (D) 20% glycerol and 50:1 molar ratio DOPC (lipid:protein).* Samples were loaded into a 1mm thermostated quartz cuvette and measured at 3°C increments. Each data point was collected for five seconds in units of mdeg, and converted to mean residue ellipticity.

Data was plotted with OrginPro 8 Software and smoothened using the Adjacent-Averaging method. The spectra demonstrate that lipid binds both DGKε-$His_{(6)}$ and DGKε Δ40-$His_{(6)}$. Heating scans were done in duplicate and averaged and the reverse scans (cooling) were performed once. Each condition was performed with samples from at least two independent purifications. Representative graphs are shown and there was little variability between independent experiments.

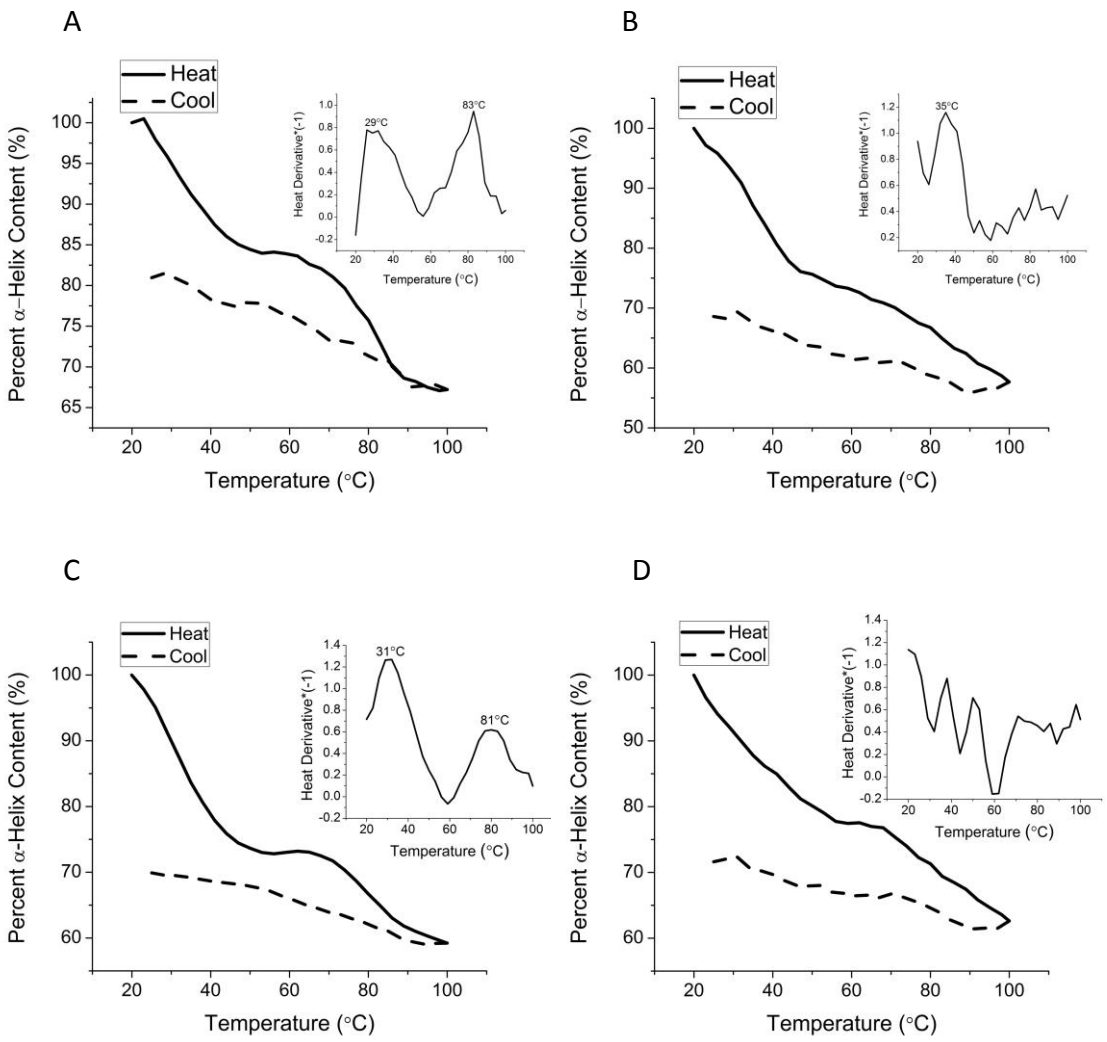

Figure 11: *Thermal denaturation of DGKε-His$_{(6)}$ with (A) 50% glycerol (B) 50% glycerol with 50:1 molar ratio DOPC (lipid:protein) and DGKε Δ40-His$_{(6)}$ with (C) 50% glycerol and (D) 50% glycerol and 50:1 molar ratio DOPC (lipid:proein).* Samples were loaded into a 1mm thermostated quartz cuvette and measured at 3°C increments. Each data point was collected for five seconds in units of mdeg, and converted to mean residue ellipticity. Data was plotted with OrginPro 8 Software and smoothened with the Adjacent-Averaging method. The spectra demonstrate that 50% glycerol facilitates the partial refolding of both DGKε-His$_{(6)}$ and DGKε Δ40-His$_{(6)}$. Heating scans were done in duplicate and averaged

and the reverse scans (cooling) were performed once. Each condition was repeated with samples from at least two independent purifications. Representative graphs are shown and there was little variability between independent experiments.

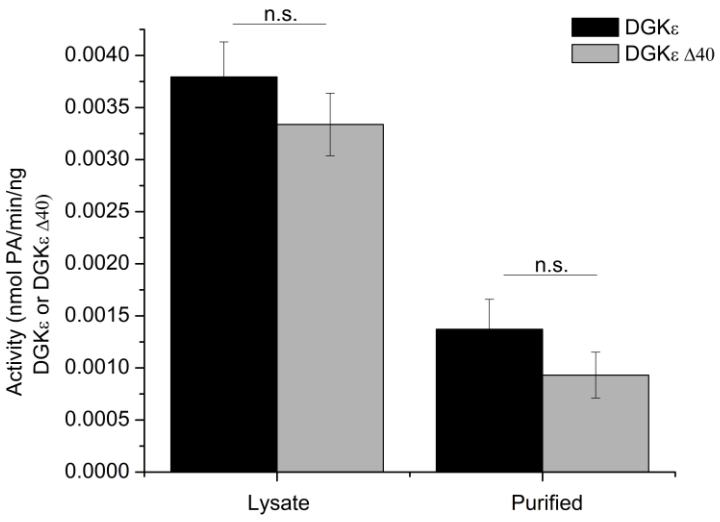

Supplementary figure 1: *Comparison of DGKε-His$_{(6)}$ and DGKε Δ40-His$_{(6)}$ activity before and after Ni-NTA purification.* The activity of Ni-NTA purified DGKε-His$_{(6)}$ and DGKε Δ40-His$_{(6)}$ relative to unpurified protein from overexpressed Sf21 cell lysates was 0.362 ± 0.108 and 0.279 ± 0.091 respectively. These results are comparable to the activity level (0.0045 nmol PA/min/ng DGKε) measured in Cos7 cell lysates (*19*).

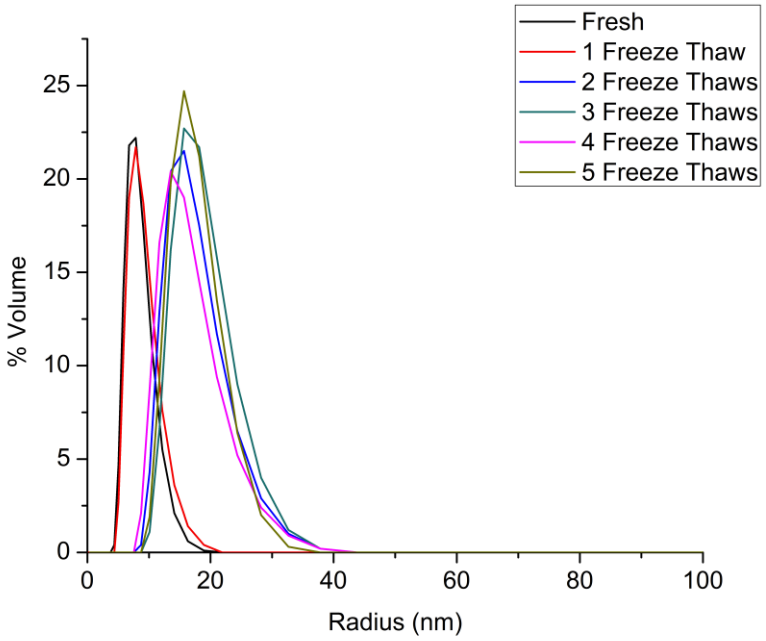

Supplementary figure 2: *Dynamic light scattering particle size distributions of DGKε-His$_{(6)}$ shown as volume distributions.* Repeated freeze thawing of Ni-NTA purified DGKε-His$_{(6)}$ increases the particle size distribution.

Tables:

	DGKε (CD)	DGKε Δ40 (CD)	dgkB[17]	DGKε[14,15,16]
α-Helix	29	30	22	25
β-Strand	22	21	34	21

Table 1: *Secondary structure comparison of DGKε, DGKε Δ40, and dgkB from Staphylococcus aureus.* The I-TASSER server prediction agrees well with the CD results, and there seems to be more β-structure in dgkB than DGKε.

CHAPTER 3: Introduction

Future Studies with Purified DGKε

This is a section discussing the impact that purifying DGKε will have on our ability to utilize a wide range of scientific techniques to study its properties. It outlines a number of experiments that have become feasible and mentions which studies are presently being pursued.

Future endeavours with purified DGKε

The successful purification of DGKε has created many interesting research opportunities and has effectively opened the door for a diverse range of research specialties to participate in its study. The availability of purified enzyme will facilitate a rapid surge in our understanding of DGKε structure and function as well as its biological importance and will undoubtedly lead to many novel discoveries.

Does DGKε interact with other proteins?

Purified DGKε preparations can be used to effectively screen for potential binding partners. Two proteins of particular interest are actin and CDS, which are currently under investigation with pull-down assays and co-immunoprecipitation experiments, respectively. DGKε has primarily been identified in the plasma membrane and the endoplasmic reticulum; however, one report has located DGKε on actin stress fibers in vascular smooth muscle cells (VSMCs) (*1*). DGKε is not the only isoform of DGK that has been associated with actin. Phosphatidylinositol 4,5-bisphosphate PIP_2 binds actin-capping proteins, releasing them and facilitating the polymerization of actin (*2;3*). DGKζ regulates PIP_2 levels by controlling phosphatidylinositol 4-phosphate 5-kinase (PIP5KI) activity via PA levels. DGKζ has also been shown to associate with proteins involved in actin dynamics (*4;5*). Additionally, DGKβ has been shown to colocalize with actin (*6*). However, the relationship between DGKε and actin is currently much less clear. An immunocytochemical study found DGKε localized on actin stress fibers in VSMCs, in contrast to DGKα which was detected sparsely in the cytoplasm and DGKζ which was observed in a granular pattern in the cell nucleus (*1*). The role of DGKε in VSMC

functions, such as contraction, proliferation, and migration is not understood. However, one observed trend is the increase of DGK activity by norepinephrine stimulation. Similarly, serotonin increases the levels of DGKε in RASMCs and causes the subcellular localization of DGKε to shift from an actin filamentous pattern to a diffuse distribution with the simultaneous disassembly of actin stress fibers (*1*). Additionally, the inhibition of Rho-associated kinases that control cytoskeletal architecture (*46*) abolishes filamentous stress fiber formation and decreases DGKε immunoreactivity on stress fibers. Serotonin elicits the same effect and suggests that DGKε is involved in the mechanisms of vasoconstriction through the regulation of stress fiber formation and/or the stability of VSMCs. It would be interesting to test the reactivity of DGKε with proteins involved in actin/cytoskeleton dynamics to better understand these findings.

Testing the reactivity of a DGK with actin polymerization proteins is exactly what one group has done with the DGKζ isoform (*4*). Phosphatidylinositol 4,5-bisphosphate (PIP_2) is produced by the type I phosphatidylinositol4-phosphate 5-kinases (PIP5KI). PIP5KI activity is regulated by PA species produced by the phosphorylation of DAG catalyzed by DGK. This gives the DGKs partial control over PIP_2 levels by regulating PIP5KI activity (*4*). DGKζ has been shown to significantly enhance PIP5KI activity in HEK293 cells. Furthermore, co-transfection of these cells with DGKζ and PIP5KI saw the co-immunoprecipitation and co-localization of these two enzymes (*4*). This study suggests that two enzymes catalyzing different steps along the phospholipid biosynthesis pathway reside in a regulated signaling complex. Employing a purification protocol like the one we developed for DGKε with the other isoforms could not only lead to their crystallization, but their co-crystallization with protein

binding partners and facilitate fascinating new discoveries. Considering that actin is widely regarded as a housekeeping protein and is expressed almost ubiquitously, and most of the DGK isoforms are not, there must be other isoforms of DGK that perform this function seen with DGKζ. The other nine DGK isoforms are more soluble and therefore could potentially be more manageable to purify and study than DGKε.

An interaction between DGKε and CDS2 would improve PI biosynthesis efficiency

A similar experimental approach to the DGKζ/PIP5Kiα studies is being developed by Epand and colleagues for investigating the possibility of an interaction between DGKε and cytidine diphosphate diacylglycerol synthase (CDS). Following DGKε catalyzed conversion of DAG to PA; CDS catalyzes the subsequent step in the PI cycle whereby PA is combined with CTP to produce CDP-DAG. DGKε is located in the PM and the ER, while CDS1 and CDS2 are found mostly in the ER. CDS and DGK catalyze sequential steps in the synthesis of PI and both are localized in the ER. Therefore, it would be logical that these two enzymes localize near one another in the same domain of the ER, if not interact directly to convert DAG→PA→ CDP-DAG in an efficient manner. This seems plausible, particularly in the case of DGKδ. DGKδ increases fatty acid synthesis giving it a critical role in the biosynthesis of many lipids (*7;45*). Similarly, CDS functions to divert CDP-DAG to PI for phospholipid synthesis during development. Therefore, it is worth investigating potential interactions between DGKδ and CDS.

DGKε exhibits the same acyl chain specificity for its substrate that the mammalian CDS2 isoform shows for its PA substrate (*8*). Since these two enzymes catalyze sequential steps in PI synthesis, it would be favorable for these two enzymes to position themselves in direct contact or in

similar domains in the ER such that the 1-stearoyl-2-arachidonoyl PA product from DGKε can be delivered directly to CDS2 without being mixed into the PA pool with the other PA species that CDS2 has no specificity for. This hypothesis could be tested *in vitro* with purified DGKε. Tagged forms of the two proteins can then be co-expressed and immunoprecipitation can be used to extract the complex from cell lysates. It would be fascinating to visualize the complex through a high resolution imaging technique such as cryo-EM or X-ray crystallography. A tremendous accomplishment would be to measure the enzymatic activity of these enzymes following their reconstitution into liposomes. This would facilitate a remarkable amount of biologically relevant information about the nature of the interactions between enzymes, enzymes and lipid membranes, and enzymes and regulatory factors. After confirming protein-protein interactions the activity of the complexes can be tested in liposomes. In theory, components of a pathway or possibly even the entire pathway can be reconstituted into a liposome system. However, there are an abundance of technical challenges that must be overcome in order to "recreate" even small components of a cycle as complex as the PI cycle. The PI cycle involves two membranes (the plasma membrane and ER membrane) and a number of the enzymes, including CDS2 are integral membrane proteins and therefore must be inserted in the proper orientation to enable function. Membrane domains necessary for supporting protein complexes would also prove immensely challenging to take into account. Regardless of the membrane protein, it is imperative to study its function in a membrane-like environment and detergent solubilized proteins are widely recognized as being rather poor models of biological membranes.

Is DGKε involved in lipid transport or membrane dynamics?

The PI cycle "begins" in the plasma membrane with the receptor-stimulated activation of PLC and involves enzymes that are localized exclusively in the ER. This fact suggests that lipids produced in the PM must be transported to the ER and vice versa. Phosphatidylinositol 4,5-bisphosphate (PIP_2) accounts for less than 1% of membrane phospholipids, yet it has a critical role in a remarkable number of cellular signalling events. These include endocytosis, cytoskeleton dynamics, store-operated Ca^{2+} entry, and GTPase, and ion transporter activity among others (9;10). As mentioned above, PIP_2 regulates actin polymerization among many other functions ranging from membrane trafficking, plasma membrane-cytoskeleton linkages, formation and regulation of clathrin-coated vesicles in endocytosis, and regulating exocytosis (*11*). The hydrolysis of PIP_2 at the cell membrane to generate DAG and inositol triphosphate governs many signaling functions, however, the mechanism facilitating its rapid replenishment following receptor-induced hydrolysis have been very unclear until recently. PI produced in the ER is required for the rapid replenishment of PM PIP_2 (*12*), however, the question has always been, how does a lipid travel through an aqueous compartment to get there? PIP_2 in the inner leaflet of the PM is generated from the successive phosphorylation of PI originating from the ER. First, PI 4-kinase phosphorylates PI to produce PI 4-phosphate (PI4P), which is the substrate for PI4P 5-kinase to yield PIP_2. Both PI 4-kinase and PI4P 5-kinase are present in the PM to generate PIP_2 from PI. However, for this to happen, PI must be delivered to the PM from the ER membrane (*9; 13*). One way this transport is accomplished is by PI transfer proteins (PITPs) (*14*). Additionally, vesicular transport has been shown to deliver PI4P form the Golgi

apparatus to the PM to replenish PIP2 levels (*15*). However, no mechanism has been identified to explain the rapid replenishment of PM PIP_2 following receptor-induced hydrolysis.

The PITP Nir2 and its homolog Nir3 have recently been shown to detect PIP_2 hydrolysis and translocate to ER-PM junctions by binding to PA. The authors demonstrated that Nir2 mediates substantial PIP2 replenishment during intense receptor stimulation, in contrast to Nir3, which senses subtle PA production in cells during times of low receptor stimulation (*12*). PA production at the PM coincides with PIP_2 hydrolysis, so detecting elevated levels of PA and delivering PI is an intricate mechanism for restoring PM PIP_2 levels. Another recently identified system for lipid transport involves moving phosphatidylserine (PS) from its location of synthesis in the ER to the PM. PS is highly enriched in the PM and contributes to negative charge and the specific recruitment of signaling proteins (*16*). The PS transporter protein Osh6p (oxysterol binding homology protein) was found to extract PI4P from the PM and exchange it for PS from the ER membrane (*16*). Crystal structures were solved of Osh6p in complex with PI4P and with PS. Interestingly, PI4P and PS do not compete with one another for binding to Osh6p, instead, they bind specifically in a mutually exclusive manner.

We speculate that DGKε may play a similar role in lipid transport between the ER membrane and PM. CDS2 exists predominantly in the ER, while DGKε is found in both the PM and ER. The Nir2 and Nir3 PI transport proteins exist at the ER-PM junctions. It seems logical that DGKε would also exist at these junctions to facilitate transport of the PA it produces in the PM to the ER membrane. It would be logical for PA enriched with stearate and arachidonate to be directly passed to CDS2 as opposed to being mixed in with the larger pool of

PA species. This could be accomplished by a direct interaction between DGKε with CDS2. Alternatively, DGKε could function as a lipid transporter or as a tether linking the PM and ER membrane. There is little evidence to support these hypotheses; currently the only known function for DGKε is DAG phosphorylation. However, using atomic force microscopy (AFM), we observed that purified DGKε and DGKε Δ40 dramatically disrupted supported lipid bilayers in a time-dependent manner. We have been able to replicate this unexpected finding as well as perform a number of control experiments to rule out the possibility of it being an artifact. We are currently testing the binding of purified DGKε to liposomes of various lipid compositions. In agreement with other studies using different isoforms, we have successfully incorporated DGKε into liposomes containing phosphatidylethanolamine. Upon finding a suitable lipid composition that supports DGKε binding we will employ leakage and fusion assays. Leakage assays will help to clarify the unexpected bilayer disruption we witnessed with AFM.

Liposome binding and activity in liposomes

The most important and physiologically relevant property of DGKε that can be measured is its enzymatic activity. Structural techniques like CD or even high-resolution methods such X-ray diffraction are very informative, however, they only indirectly provide information about function. Even if the CD spectra of a purified sample reveals proper folding it cannot be concluded that the sample is capable of effectively catalyzing the reaction that it is expected to in biologically relevant conditions. Currently, the best method for measuring the enzymatic activity of DGKε is the detergent/phospholipid mixed-micelle activity assay, which has many disadvantages. Lipids in the micellar form, as opposed to the bilayer or liposomal form,

resemble biological membranes much less closely. The lipids comprising a liposome can be manipulated to imitate various biological membranes, like the cytoplasmic versus extracellular leaflet of the plasma membrane, or one of the leaflets from a raft domain. Furthermore, substituting different lipids and cholesterol allows for testing the effects of curvature properties (*17*). More complex bilayers with asymmetric distributions of lipid constituents can also be created (*18*). The liposome-based assay more closely resembles the conditions of a cell membrane and is a superior means for assessing enzyme function. For example, studies with PKC show that liposomal assays exhibit greater sensitivity to modulators of enzymatic activity compared with micelle-based assays (*19*). Therefore, it is clear that a liposome based assay or an alternative membrane-like system must be developed to make biologically relevant conclusions about DGKε function.

A liposome-based assay was previously used to study two of the DGK isoforms: DGKα and DGKζ (*17;20*). DGKα and DGKζ were not purified; instead they were recovered by salt extractions. This cruder preparation still provided valuable information regarding the role of lipids in altering the activity and specificity of DGKα (*17;20*). Studies in micelles fail to show consistent relationships between the physical properties of the phospholipids added to the outcome on DGK activity (*20*). However, in a liposome-based system, DGKα and DGKζ show a marked increase in activity in response to negative membrane curvature promoting lipids (*20*). The observed lack of sensitivity to membrane curvature by membrane proteins in a micellar system is due to the overwhelming tendency of the detergent to induce positive

curvature (*20*). These studies demonstrate that the sensitivity of DGK to changes in lipid composition is much more sensitive in liposomes compared to detergent micelles (*20*).

Liposomes mimic a membrane-like environment for studying DGK's

One liposome study demonstrated that the substrate specificity of a DGK depends not simply on the particular acyl chains but also on the nature of the lipid head group (*17*). These studies also show that the nature of the substrate specificity is also dependent on the nature of the surrounding lipids present in the liposome. Liposomes comprised of lipids with less hydration and more intrinsic negative membrane curvature reduced the selectivity of DGKα for 1-O-hexanoyl-2-arachidonoylglycerol (HAG) over 1-O-hexanoyl-2-oleoylglycerol (HOG). DGKα and DGKζ activity was measured in liposomes under a variety of different conditions revealing a number of important findings with biological significance (*17;20*). The diversity of molecular species that exists for a lipid with one particular headgroup is enormous especially considering the number of carbons and degrees of unsaturation that are possible (*21*). With respect to the DGK's, much more attention has been given to substrate specificity with respect to the acyl chains. This liposome study compared substrates with ester versus ether linkages at the sn-1 position of glycerol. Ether containing glycerol derivatives are derived from alkyl ester lipids, such as the plasmalogens (*17*). The plasmalogens make up a significant fraction of the phosphatidylcholine and phosphatidylethanolamine present in the plasma membrane (*22*). Estimates suggest upwards of one half of the phospholipids present in the cytoplasmic leaflet of raft domains are alkyllipids (*23*). Furthermore, acyl and alkyl linked lysophosphatidic acids have been shown to elicit different responses in human platelets (*24*). The liposome studies

showed that DGKα and DGKζ prefer the DAG substrates to alkyl acylglycerol (AAG) substrates. Curiously, DGKα and DGKζ showed specificity for HAG over HOG. DGKα and DGKζ do not discriminate species of DAG. Both cholesterol and PE were found to reduce the substrate specificity of DGKα and DGKζ. The authors did not test DGKε activity in liposomes. It would be interesting to test if the liposome system changes DGKε's substrate specificity properties. These studies with a liposome-based assay were sensitive to changes in lipid and suggest the importance of conducting similar experiments with DGKε.

Liposome studies previously done with DGKα and DGKζ reveal important findings that we are currently applying to our liposome studies with DGKε. PE increased the partitioning of DGKα and DGKζ to the liposomes and inceased the catalytic rate of the membrane-bound enzyme (*20*). We have also shown that DGKε binds preferably to liposomes comprised of PE. Studies showed that cholesterol, which we have not yet tested with DGKε, elicited a similar activating effect on DGKα and DGKζ as PE. Similar to PE, cholesterol induces negative curvature stress in membranes. These studies are the first to illustrate that lipid species which increase the propensity of the liposome to form inverted phases are activators of DGK. Testing the effects of cholesterol on DGKε is important because DGKε possesses a cholesterol recognition amino acid consensus (CRAC) motif. It is plausible that cholesterol would be required for DGKε activity; however, the enzyme is active in micelle systems lacking cholesterol. DGKε and mutants with either a deleted CRAC motif or different point mutations could be tested in a liposome-based assay to help clarify this matter. Sphingomyelin and cholesterol are both major constituents in the controversial raft domains that are believed to

function as signaling platforms for a variety of signaling cascades. Sphingomyelin was shown to have a strongly inhibit both DGKα and DGKζ. This makes their effect on enzyme activity particularly relevant.

DGKα possesses a Ca^{2+} binding EF-hand motif. Studies with the wild-type DGKα and a variety of truncated forms lacking the calcium binding EF-hand motif have lead to the conclusion that DOPE and cholesterol activate DGKα by inducing a conformational change that makes the active site accessible in a mechanism similar to calcium (*20*). Similar strategies can be used to investigate the role of cholesterol and other modulators on DGKε activity. These studies show the ability of liposomal studies to effectively illustrate that membrane proteins are modulated by the composition and properties of the lipid milieu in which they are embedded (*20*).

Nanodisks as model membranes for studying membrane proteins

The ATP binding cassette reporter MsbA uses the energy from ATP hydrolysis to transport substrates across membranes. Until recently, MsbA has only been studied in detergent-based micelles (*25*). MsbA is present in the inner leaflet of gram-negative bacteria where it transports lipid species from the inner to the outer leaflet (*26*). ATP-binding cassette (ABC) transporters have a general core structure comprising two transmembrane domains that form a translocation pathway as well as two conserved nucleotide-binding domains (NBDs) that bind and hydrolyze ATP. Upon ATP binding to each NBD, a NBD dimerization occurs and is required for ATP hydrolysis. Upon hydrolysis of one of the molecules of ATP, the dimer

dissociates in a manner that is coupled to rearrangements of the transmembrane helices from an inward-facing conformation to an outward-facing conformation with the concomitant translocation of substrate. Crystal structures exist for both the inward and outward facing conformations of MsbA. In addition to crystal structure data, several spectroscopic techniques also suggest large motions between the two conformations. This is in contrast to the results obtained under more the more physiologically relevant conditions achieved with reconstitution into nanodiscs.

Nanodiscs are self-assembled structures encased with a membrane scaffolding protein (MSP). The ATPase activity of MsbA was 10-fold higher when reconstituted into nanodiscs compared to detergent solubilization (*25*). The authors stress the importance of performing structural and functional studies of membrane proteins under physiological temperatures and native-like conditions. They suggest that certain experimental conditions, such as crystallization may lock the protein in a rare conformation, in the case of MsbA, where the nucleotide binding domains (NBDs) are farther apart from each other. The authors used luminescence resonance energy transfer spectroscopy to study MsbA reconstituted in nanodiscs at physiological temperatures while it catalyzes ATP hydrolysis. MsbA was compared to data collected with double electron-electron resonance and x-ray crystallography. They recorded a significantly smaller distance between the nucleotide-binding domains and a larger fraction of molecules with nucleotide-binding domains in the nucleotide-free state under more biological conditions (*26*). This example stresses the importance of studying DGKε in a membrane-like environment

with as close to biological conditions as possible, it also suggests that structural results must be analyzed critically before drawing conclusions.

Phospholipid bicelles improve the conformational stability of membrane proteins

The visual photoreceptor rhodopsin (Rho) is a typical member of the GPCR superfamily. Mutations to Rho are one of the main causes of the retinitis pigmentosa disorder that leads to rod photoreceptor cell death and eventually blindness (*27*). Structural and functional characterization of this receptor is typically conducted in a detergent solution of dodecyl maltoside (*28*). There are numerous examples of membrane proteins showing poor conformational stability in detergent micelles (*29*). With respect to Rho, bicelles have been shown to improve its stability. In contrast to detergents, lipid bilayers increase the stability and facilitate the folding, assembly, and function of a wide variety of membrane proteins (*30;31*). The stability of two Rho mutants relevant to RP retinal disease was studied in DMPC/DHPC bicelles (*32*). One of the mutants showed a significant increase in the chromophore thermal stability and regeneration, the other mutant showed improved thermal stability but no improvement in its retinal regeneration ability. The different stability properties of Rho mutants that manifest in different phenotypes provide insight into the development of targeted therapies toward retinal degenerative diseases. These properties are much more sensitive to analysis in micelle systems, which emphasize the importance of upgrading the DGKε mixed-micelle activity assay.

The structures of prokaryotic DGKs have been solved

Bacteria possess two DGK encoding genes: *dgkA* and *dgkB.* The *dgkA* gene encodes dgkA in gram-negative bacteria and primarily undecaprenol kinase (UDPK) in gram-positive bacteria (*33*). DgkA and UDPK are very hydrophobic and uncommonly small kinases that share very little homology with the eukaryotic DGKs and their prokaryotic homologs encoded by the *dgkB* gene (*34*). There has been considerably more progress in characterizing the prokaryotic DGK enzymes. DgkA and UDPK are insoluble integral membrane proteins with three membrane-spanning alpha helices that function as homotrimers comprising a total of nine membrane-spanning alpha helices and three active sites (*35*). The structure of dgkA was determined by solution NMR (*35*) and later by crystallography (*36*). It has been demonstrated that its structure is quite thermodynamically and kinetically stable (*35*).

The crystal structure of dgkB was determined in 2008 and shows no resemblance to dgkA (*37*). Instead, the water-soluble enzyme from gram-positive bacteria shares sequence homology between key active site residues within its catalytic domain and the catalytic cores of the mammalian DGKs (*37;38*). DGKε and dgkB share a two-domain architecture and the conserved catalytic domain residues between these two proteins indicate that they likely function with a similar mechanism and have a similar structure. Unfortunately, there are no structures reported for any of the mammalian isoforms to determine if the observed sequence homology between these two enzymes confers structural similarities.

Structural information is lacking for mammalian DGK isoforms

A robust method for expressing large quantities of DGKε is required to characterize DGKε adequately and the inability to do this has been a major reason why this enzyme has not been purified until recently. We have experienced great difficulty developing an appropriate expression system. Recombinant human DGKε expresses very well in bacteria; however, it is not active, making it irrelevant for activity studies. Furthermore, there is only one report of a human DGK being successfully expressed in yeast (*39*) and we have had little success with yeast ourselves. We have unsuccessfully attempted to over express DGKε in a strain of yeast that had been genetically modified to produce cholesterol instead of ergosterol (*40*). Neither yeast nor bacteria produce cholesterol, which has well documented functions in cell membranes. We speculated that the absence of cholesterol in yeast and bacteria could be a contributing factor to their inability to express active DGKε. We were unable to detect expression with this system; however, different vectors and growth conditions could be tested to fully eliminate this strain as an option. We have previously shown that DGKε can be over-expressed in insect (Sf21) cells (*41*) and that the enzymatic activity of Sf21 cells lysates over expressing DGKε is comparable to the activity of DGKε transfected Cos7 cells. Our recent success in purifying human DGKε and a truncated form lacking the first 40 residues (DGKεΔ40) is a critical step towards obtaining high-resolution structural data. We showed that both purified constructs retained their substrate acyl chain specificity and have a specific activity comparable to N-terminally FLAG epitope tagged forms of these proteins expressed in Cos-7 cells. Thus, the purified protein recovered from our protocol is biologically relevant and suitable for both enzymatic and structural studies.

The primary amino acid sequence of DGKε suggests that the protein has a two-domain architecture, similar to dgkB from gram-positive bacteria (*42*). The domain of DGKε that houses the catalytic site is homologous to the first domain of dgkB, while the other domain seems to have evolved separately (*42*). A two-domain structure agrees with our CD finding that DGKε possesses two distinct thermal transitions (Jennings et al., 2016, submitted). Full-length dgkB has been crystallized, so it seems promising that at least the catalytic domain of DGKε could be crystallized under similar conditions. This would be especially worth trying if the fully intact wild-type protein proves to be a challenge. This accomplishment would lead to a better understanding of the interaction between DGKε and its substrate, as well as clarify the mechanism underlining DGKε's unique substrate specificity. Cryo EM may also be used to visualize DGKε on liposomes. If co-immunoprecipitation experiments with other enzymes are successful, the resulting protein complexes could be studied with this method and/or with crystallography.

Designing an isoform-specific inhibitor for DGKε

A detailed crystal structure of DGKε would be invaluable in the design of a specific inhibitor. Recently, the first isoform specific inhibitor was developed for DGKα (*43*). This isoform has attracted attention for its role in cancer cell proliferation and immunity (*43*). A large library of chemical compounds was screened using a newly established, high-throughput DGK assay (*44*). The authors demonstrated that their compound is a potent and specific inhibitor of DGKα activity, whereby it targets the catalytic region and disrupts ATP binding.

The outcome attenuated cancer cell proliferations and enhanced anticancer immunity in a human hepatocellular carcinoma cell line (*43*). A similar study with DGKε would have important implications in diseases such as atypical hemolytic uremic syndrome, Huntington's disease, and epilepsy. Given the importance of the lipid environment, membrane composition, and temperature for membrane protein structure and function it is critical that the assay for DGKε activity used to screen for novel inhibitors be adapted to resemble a more membrane-like environment; otherwise the results may be irrelevant. Epand and colleagues have begun adapting the assay used to develop the DGKα inhibitor for DGKε. The success of this project will contribute to discerning the intracellular functions and physiological importance of this isoform and potentially lead to therapies for a number of DGKε-related pathologies.

References

1. Nakano, T., Hozumi, Y., Goto, K., & Wakabayashi, I. (2009). Localization of diacylglycerol kinase ε on stress fibers in vascular smooth muscle cells. *Cell and tissue research*, *337*(1), 167-175.

2. Toker, A. (1998). The synthesis and cellular roles of phosphatidylinositol 4, 5-bisphosphate. *Current opinion in cell biology*, *10*(2), 254-261.

3. Yin, H. L., & Janmey, P. A. (2003). Phosphoinositide regulation of the actin cytoskeleton. *Annual review of physiology*, *65*(1), 761-789.

4. Luo, B., Prescott, S. M., & Topham, M. K. (2004). Diacylglycerol kinase ζ regulates phosphatidylinositol 4-phosphate 5-kinase Iα by a novel mechanism. *Cellular signalling*, *16*(8), 891-897.

5. Abramovici, H., Mojtabaie, P., Parks, R. J., Zhong, X. P., Koretzky, G. A., Topham, M. K., & Gee, S. H. (2009). Diacylglycerol kinase ζ regulates actin cytoskeleton reorganization through dissociation of Rac1 from RhoGDI. *Molecular biology of the cell*, *20*(7), 2049-2059.

6. Kobayashi, N., Hozumi, Y., Ito, T., Hosoya, T., Kondo, H., & Goto, K. (2007). Differential subcellular targeting and activity-dependent subcellular localization of

diacylglycerol kinase isozymes in transfected cells. *European journal of cell biology*, *86*(8), 433-444.

7. Shulga, Y. V., Topham, M. K., & Epand, R. M. (2011). Regulation and functions of diacylglycerol kinases. *Chemical reviews*, *111*(10), 6186-6208.

8. D'Souza, K., Kim, Y. J., Balla, T., & Epand, R. M. (2014). Distinct properties of the two isoforms of CDP-diacylglycerol synthase. *Biochemistry*, *53*(47), 7358-7367.

9. Balla, T. (2013). Phosphoinositides: tiny lipids with giant impact on cell regulation. *Physiological reviews*, *93*(3), 1019-1137.

10. Di Paolo, G., & De Camilli, P. (2006). Phosphoinositides in cell regulation and membrane dynamics. *Nature*, *443*(7112), 651-657.

11. Czech, M. P. (2000). PIP2 and PIP3: complex roles at the cell surface. *Cell*, *100*(6), 603-606.

12. Chang, C. L., & Liou, J. (2015). Phosphatidylinositol 4, 5-bisphosphate homeostasis regulated by Nir2 and Nir3 proteins at endoplasmic reticulum-plasma membrane junctions. *Journal of Biological Chemistry*, *290*(23), 14289-14301.

13. Nakatsu, F., Baskin, J. M., Chung, J., Tanner, L. B., Shui, G., Lee, S. Y., ... & De Camilli, P. (2012). PtdIns4P synthesis by PI4KIIIα at the plasma membrane and its impact on plasma membrane identity. *The Journal of cell biology*, *199*(6), 1003-1016.

14. Lev, S. (2012). Nonvesicular lipid transfer from the endoplasmic reticulum. *Cold Spring Harbor perspectives in biology*, *4*(10), a013300.

15. Dickson, E. J., Jensen, J. B., & Hille, B. (2014). Golgi and plasma membrane pools of PI (4) P contribute to plasma membrane PI (4, 5) P2 and maintenance of KCNQ2/3 ion channel current. *Proceedings of the National Academy of Sciences*, *111*(22), E2281-E2290.

16. von Filseck, J. M., Čopič, A., Delfosse, V., Vanni, S., Jackson, C. L., Bourguet, W., & Drin, G. (2015). Phosphatidylserine transport by ORP/Osh proteins is driven by phosphatidylinositol 4-phosphate. *Science*, *349*(6246), 432-436.

17. Epand, R. M., Kam, A., Bridgelal, N., Saiga, A., & Topham, M. K. (2004). The α isoform of diacylglycerol kinase exhibits arachidonoyl specificity with alkylacylglycerol. *Biochemistry*, *43*(46), 14778-14783.

18. Marquardt, D., Geier, B., & Pabst, G. (2015). Asymmetric lipid membranes: towards more realistic model systems. *Membranes*, *5*(2), 180-196.
19. Mosior M., and R.M. Epand. (1994). Characterization of the calcium-binding site that regulates association of protein kinase C with phospholipid bilayers. *J. Biol. Chem.*, v.269, p.13798.
20. M.L. Fanani, M.K. Topham, J.P. Walsh, R.M. Epand. (2004). Lipid modulation of the activity of diacylglycerol kinase alpha- and zeta-isoforms: activation by phosphatidylethanolamine and cholesterol. *Biochemistry*, 43 (2004), pp. 14767–14777.
21. Kimura, T., Jennings, W., & Epand, R. M. (2016). Roles of specific lipid species in the cell and their molecular mechanism. *Progress in lipid research*, *62*, 75-92.
22. Nagan, N., & Zoeller, R. A. (2001). Plasmalogens: biosynthesis and functions. *Progress in lipid research*, *40*(3), 199-229.
23. Pike, L. J., Han, X., Chung, K. N., and Gross, R. W. (2002) Lipid rafts are enriched in arachidonic acid and plasmenylethanolamine and their composition is independent of caveolin-1 expression: a quantitative electrospray ionization/mass spectrometric analysis, *Biochemistry.* 41, 2075-2088.
24. Tokumura, A., Sinomiya, J., Kishimoto, S., Tanaka, T., Kogure, K., Sugiura, T.,

Satouchi, K., Waku, K., and Fukuzawa, K. (2002). Human platelets respond differentially to lysophosphatidic acids having a highly unsaturated fatty acyl group and alkyl ether-linked lysophosphatidic acids, *Biochem. J*. 365, 617-628.

25. Zoghbi, M. E., Cooper, R. S., & Altenberg, G. A. (2016). The lipid bilayer modulates the structure and function of an ATP-binding cassette exporter. *Journal of Biological Chemistry*, *291*(9), 4453-4461.

26. Doerrler, W. T., Gibbons, H. S., and Raetz, C. R. (2004). MsbA-dependent translocation of lipids across the inner membrane of Escherichia coli. *J. Biol. Chem*. 279, 45102–45109.

27. Daiger, S. P., Sullivan, L. S., and Bowne, S. J. (2013). Genes and mutations causing retinitis pigmentosa. *Clin. Genet*. 84, 132−141.

28. Ramon, E., Marron, J., del Valle, L., Bosch, L., Andres, A., Manyosa, J., and Garriga, P. (2003). Effect of dodecyl maltoside detergent on rhodopsin stability and function. *Vision Res*. 43, 3055−3061.

29. Tsukamoto, H., Szundi, I., Lewis, J. W., Farrens, D. L., and Kliger, D. S. (2011). Rhodopsin in nanodiscs has native membrane-like photointermediates. *Biochemistry*, 50, 5086−5091.

30. Saliba, R. S., Munro, P. M. G., Luthert, P. J., and Cheetham, M. E. (2002). The cellular fate of mutant rhodopsin: quality control, degradation and aggresome formation. *Journal of cell science*, 115, 2907−2918.

31. Sanders, C. R., and Prosser, R. S. (1998). Bicelles: a model membrane system for all seasons? *Structure* (Oxford, U. K.) 6, 1227−1234.

32. Dong, X., Ramon, E., Herrera-Hernández, M. G., & Garriga, P. (2015). Phospholipid bicelles improve the conformational stability of rhodopsin mutants associated with retinitis pigmentosa. *Biochemistry*, *54*(31), 4795-4804.

33. Jerga, A., Lu, Y. J., Schujman, G. E., de Mendoza, D., & Rock, C. O. (2007). Identification of a soluble diacylglycerol kinase required for lipoteichoic acid production in Bacillus subtilis. *Journal of Biological Chemistry*, *282*(30), 21738-21745.

34. Van Horn, W. D., & Sanders, C. R. (2012). Prokaryotic diacylglycerol kinase and undecaprenol kinase. *Annual review of biophysics*, *41*, 81.

35. Van Horn, W. D., Kim, H. J., Ellis, C. D., Hadziselimovic, A., Sulistijo, E. S., Karra, M. D., ... & Sanders, C. R. (2009). Solution nuclear magnetic resonance structure of membrane-integral diacylglycerol kinase. *Science*, *324*(5935), 1726-1729.

36. Li, D., Lyons, J. A., Pye, V. E., Vogeley, L., Aragão, D., Kenyon, C. P., ... & Caffrey, M. (2013). Crystal structure of the integral membrane diacylglycerol kinase. *Nature*, *497*(7450), 521-524.

37. Miller, D. J., Jerga, A., Rock, C. O., & White, S. W. (2008). Analysis of the Staphylococcus aureus DgkB structure reveals a common catalytic mechanism for the soluble diacylglycerol kinases. *Structure*, *16*(7), 1036-1046.

38. Jerga, A., Miller, D. J., White, S. W., & Rock, C. O. (2009). Molecular determinants for interfacial binding and conformational change in a soluble diacylglycerol kinase. *Journal of Biological Chemistry*, *284*(11), 7246-7254.

39. Abe, T., Lu, X., Jiang, Y., Boccone, C. E., Qian, S., Vattem, K. M., Wek, R. C., and Walsh, J. P. (2003) Site-directed mutagenesis of the active site of diacylglycerol kinase alpha: calcium and phosphatidylserine stimulate enzyme activity via distinct mechanisms, *Biochem. J. 375*, 673-680.

40. Souza, C. M., Schwabe, T. M., Pichler, H., Ploier, B., Leitner, E., Guan, X. L., ... & Riezman, H. (2011). A stable yeast strain efficiently producing cholesterol instead of ergosterol is functional for tryptophan uptake, but not weak organic acid resistance. *Metabolic engineering*, *13*(5), 555-569.

41. Prodeus, A., Berno, B., Topham, M. K., & Epand, R. M. (2013). The basis of the substrate specificity of the epsilon isoform of human diacylglycerol kinase is not a consequence of competing hydrolysis of ATP. *Chemistry and physics of lipids*, *166*, 26-30.

42. Jennings, W., Doshi, S., D'Souza, K., & Epand, R. M. (2015). Molecular properties of diacylglycerol kinase-epsilon in relation to function. *Chemistry and physics of lipids*, *192*, 100-108.

43. Liu, K., Kunii, N., Sakuma, M., Yamaki, A., Mizuno, S., Sato, M., ... & Okabe, T. (2016). A novel diacylglycerol kinase α-selective inhibitor, CU-3, induces cancer cell apoptosis and enhances immune response. *Journal of lipid research*, *57*(3), 368-379.

44. Sato, M., Liu, K., Sasaki, S., Kunii, N., Sakai, H., Mizuno, H., ... & Sakane, F. (2013). Evaluations of the selectivities of the diacylglycerol kinase inhibitors R59022 and R59949 among diacylglycerol kinase isozymes using a new non-radioactive assay method. *Pharmacology*, *92*(1-2), 99-107.

45. Shulga, Y. V., Loukov, D., Ivanova, P. T., Milne, S. B., Myers, D. S., Hatch, G. M., ... & Topham, M. K. (2013). Diacylglycerol kinase delta promotes lipogenesis. *Biochemistry*, *52*(44), 7766-7776.

46. McBeath, R., Pirone, D. M., Nelson, C. M., Bhadriraju, K., & Chen, C. S. (2004). Cell shape, cytoskeletal tension, and RhoA regulate stem cell lineage commitment. *Developmental cell*, *6*(4), 483-495.